iScience

CellPress
OPEN ACCESS

Review

Targeting implant-associated infections: titanium surface loaded with antimicrobial

João Gabriel Silva Souza,[1,2,3] Martinna Mendonça Bertolini,[4] Raphael Cavalcante Costa,[1] Bruna Egumi Nagay,[1] Anna Dongari-Bagtzoglou,[4] and Valentim Adelino Ricardo Barão[1,*]

SUMMARY

Implant devices have = proven a successful treatment modality in reconstructive surgeries. However, increasing rates of peri-implant diseases demand further examination of their pathogenesis. Polymicrobial biofilm formation on titanium surfaces has been considered the main risk factor for inflammatory processes on tissues surrounding implant devices, which often lead to implant failure. To overcome microbial accumulation on titanium surfaces biofilm targeting strategies have been developed to modify the surface and incorporate antimicrobial coatings. Because antibiotics are widely used to treat polymicrobial infections, these agents have recently started to be incorporated on titanium surface. This review discusses the biofilm formation on titanium dental implants and key factors to be considered in therapeutic and preventative strategies. Moreover, a systematic review was conducted on coatings developed for titanium surfaces using different antibiotics. This review will also shed light on potential alternative strategies aiming to reduce microbial loads and control polymicrobial infection on implanted devices.

INTRODUCTION

Titanium (Ti) has been used as the main biomaterial for orthopedic and dental implant devices due to its excellent physical-chemical properties and high biocompatibility with host tissues that promote predictable long-term treatment (Spriano et al., 2018). Nonetheless, once exposed to the external environment, implants are also exposed to microbial adhesion and biofilm formation (Lang et al., 1993; Marsh et al., 2011; Mombelli and Décaillet 2011), which ultimately can trigger local inflammation in the surrounding tissues (Arciola et al., 2018).

Polymicrobial biofilm infections are the main reason for dental implant failure, which is associated with an exacerbated inflammatory response followed by significant tissue damage, resulting in loss of supporting structures (Nguyen et al., 2017). Progressive biofilm maturation and polymicrobial community assembly often result in increased virulence (Costerton et al., 1995; Flemming and Wingender, 2010; Bowen et al., 2018), and this process has been implicated as a critical factor in the pathogenesis of biofilm infections (Bowen et al., 2018). Although a host inflammatory response aiming to activate immune functions and control the microbial growth is present, this process can also result in a hypervirulent and multidrug-tolerant biofilm (Marsh and Devine, 2011). Such biofilms are challenging to treat due to their complex microbial composition and tridimensional structure (Flemming and Wingender, 2010; Arciola et al., 2018). This fact may explain the lack of consensus regarding the effective treatment strategies for oral implant-related infections (Heitz-Mayfield and Mombelli, 2014).

Although oral biofilm formation has been widely explored in the literature, it has been focused mainly on dental surfaces (Bowen et al., 2018). However, in recent years, dental implants have been widely used in the replacement of missing teeth, and therefore, their different surface properties, which directly affect biologic responses and microbial adhesion, must be considered in developing therapeutic strategies related to biofilm removal (Song et al., 2015; Souza et al., 2020a, 2020b). Therefore, the knowledge we gained on biofilm formation on oral surfaces cannot be simply transferred to implant surfaces. To overcome microbial accumulation on Ti surfaces some anti-biofilm strategies have been developed, mainly focused on surface properties and antimicrobial coatings (Song et al., 2015; Ferraris and Spriano, 2016).

[1]Department of Prosthodontics and Periodontology, Piracicaba Dental School, University of Campinas (UNICAMP), Piracicaba, São Paulo 13414-903, Brazil

[2]Dental Research Division, Guarulhos University, Guarulhos, SP 07023-070, Brazil

[3]Dentistry Science School (Faculdade de Ciências Odontológicas - FCO), Montes Claros, Minas Gerais, 39401-303, Brazil

[4]Department of Oral Health and Diagnostic Sciences, University of Connecticut Health Center, Farmington, CT 06030, USA

*Correspondence: vbarao@unicamp.br

https://doi.org/10.1016/j.isci.2020.102008

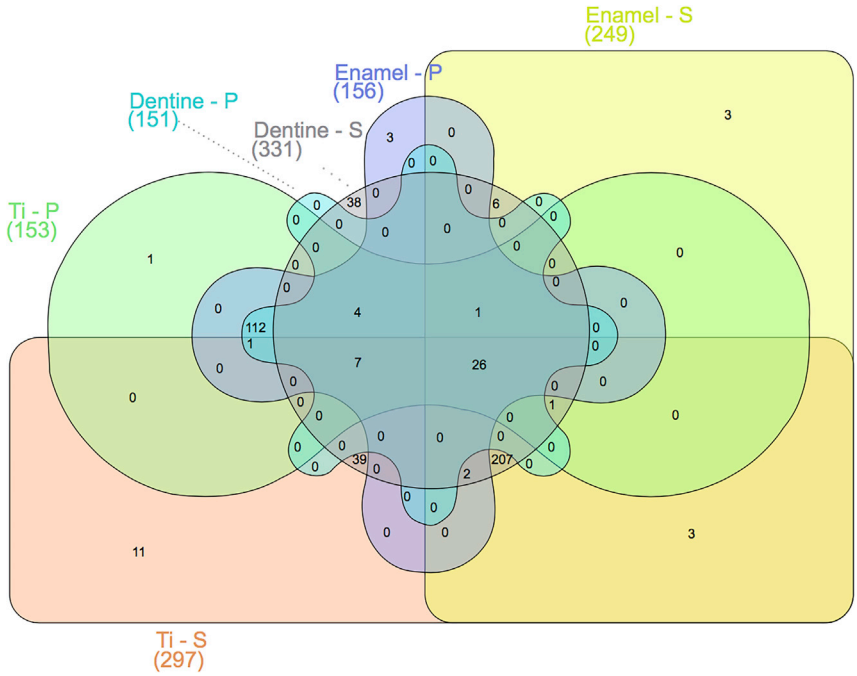

Figure 1. Venn diagram of proteins adsorbed on titanium (Ti), enamel, and dentine surfaces from saliva (S) and plasma (P)

Surfaces were exposed to human stimulated saliva or human plasma for 2 h at 35°C in an orbital shaker (70 rpm) and evaluated by liquid chromatography coupled with tandem mass spectrometry (LC–MS/MS). Numbers in parentheses are total proteins identified in each surface. Although there are shared proteins among the surfaces and in the different fluids (saliva and plasma), all groups/surfaces showed unique proteins adsorbed, showing the effect of chemical and physical properties of substrate to modulate protein adsorption.

Several antimicrobial molecules, compounds, and ions were functionalized on Ti material to reduce viable microorganisms in biofilms forming on the surface (Ferraris and Spriano, 2016; Chouirfa et al., 2019). Because antibiotics have been used to treat polymicrobial infections, including oral infections, these agents have also been loaded on Ti surfaces as a coating layer, aiming to provide bactericidal and/or bacteriostatic effect (Darouiche, 2004; Davidson et al., 2015; Stevanović et al., 2020). Even though this may be a promising approach to control microbial accumulation on implanted devices, such strategies must be developed using agents and conditions that do not damage the physical-chemical properties of Ti surface, so that biocompatibility with oral tissues can be maintained. This review aims to discuss the biofilm formation process on Ti material and key factors to be considered by therapeutic strategies using antibiotic agents loaded on surfaces, focusing on current and emergent biofilm control strategies.

Polymicrobial biofilm formation on titanium surfaces

Protein adsorption on implanted biomaterial is considered the first biologic response immediately after implantation in the human body. In the oral environment, both saliva present at the supragingival level and blood plasma at the subgingival level are protein-rich fluids in contact with dental implant devices (Lendenmann et al., 2000; Rabe et al., 2011). The protein layer adsorbed on implant surfaces is responsible for mediating subsequent cellular events, such as microbial and host cell adhesion (Kalasin and Santore, 2009; Rabe et al., 2011; Bürgers et al., 2018) as well as the osseointegration process of dental implants (Romero-Gavilán et al., 2017). Importantly, our group and others have shown that the chemical composition and topography of Ti surfaces affect the proteomic profile of proteins adsorbed from saliva and plasma (Dodo et al., 2013; Pantaroto et al., 2019; Souza et al., 2020a). Moreover, Lima et al. (2008) showed that the pellicle protein composition on Ti surfaces is different compared with hydroxyapatite surfaces (main mineral of tooth enamel), confirming the effect of different material surfaces in the oral environment in modulating protein adsorption. In fact, our unpublished work showed differences in the proteomic profile of proteins adsorbed after 2 h from saliva versus plasma on Ti, enamel, and dentine surfaces (Figure 1). Interestingly, we observed differences not only between saliva and plasma but also among the different substrates tested.

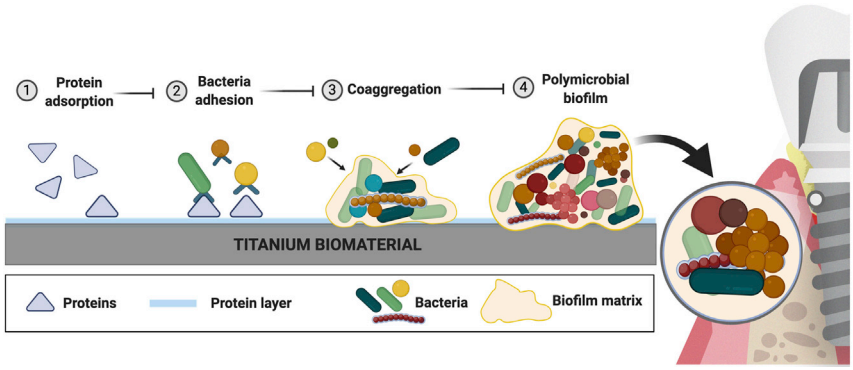

Figure 2. Steps of biofilm formation on titanium biomaterial

Dental implant surfaces made of titanium biomaterial provide the substrate for polymicrobial biofilm formation in the oral environment. Titanium surface is immediately coated by proteins from saliva (supra-mucosal segment) and plasma (sub-mucosal segment) after implant insertion. (1) Protein adsorption on the surface forms a layer with a composition directly affected by the chemical and physical properties of the surface. This layer is the main mediator of microbial adhesion through adhesin-receptor interactions. (2) Initial colonizers, mainly *Streptococcus* species, adhere on the surface binding to the protein layer. (3) Subsequently, co-aggregation processes and interaction between different species promote biofilm accumulation. (4) This synergistic interaction among organisms continues to contribute to the biofilm structure. These microbial communities are gradually embedded in the extracellular matrix, formed mainly by exopolysaccharides, eDNA, and proteins. This biofilm environment (structure) enhances the microbial interaction and cooperation, antimicrobial resistance, and nutrients/biomolecule retention-diffusion (created by BioRender®).

Protein adsorption on surfaces is the first step preceding microbial accumulation and the main mediator of oral microbial adhesion (Whittaker et al., 1996; Rabe et al., 2011). Oral bacteria can adhere on natural oral surfaces or on the surface of any material placed in the mouth, once it is coated with saliva/serum proteins. Thus, the human oral cavity provides a unique environment for microbial adhesion and polymicrobial aggregation hosting close to a thousand of bacterial species detectable by high-throughput 16S rRNA gene sequencing (Dewhirst et al., 2010; Welch et al., 2019). Even though Firmicutes, Proteobacteria, Actinobacteria, Bacteroidetes, and Fusobacteria have been described as the most abundant taxa in the oral cavity (Zaura et al., 2009), it is known that different intraoral niches harbor distinct bacterial communities, with unique sequences for different niches (Zaura et al., 2009). The recognition of protein pellicle receptors by early colonizing bacteria (second step of biofilm formation) allows the selection of certain microbial species accumulation on exposed surfaces (Kolenbrander et al., 2006). These early colonizers, in the dental surfaces, are mostly composed by *Streptococcus, Actinomyces, Gemella, Granulicatella, Neisseria, Prevotella, Rothia, and Veillonella* species (Kolenbrander et al., 2006). However, in dental implants *Streptococcus*, *Fusobacterium*, and *Capnocytophaga* species have been reported to be more abundant on the surface immediately after implant insertion (Fürst et al., 2007), suggesting some differences when compared with dental surfaces. After initial microbial adhesion, interactions among different species known as co-aggregation (third step of biofilm formation) are proposed to drive the maturation of the biofilm structure. In this way, a specific process of co-aggregation takes place where each strain co-aggregates with a specific set of strains in a well-orchestrated bacterial succession, which results in the incorporation of late colonizers in the biofilm (Kolenbrander et al., 2006). The structure formed is a polymicrobial biofilm, which is characterized by microbial communities enmeshed in a three-dimensional (3D) extracellular matrix attached to a surface (Costerton et al., 1995; Koo et al., 2013). This structure has specific characteristics that promotes microbial growth, creating a well-established and stable "climax community" (Step 4 of biofilm formation) that thrives within its microenvironment in which they have ideal physicochemical conditions, increased virulence, and antibiotic resistance (Socransky and Haffajee, 2002; Marsh et al., 2011) (Figure 2).

Even though initial differences are seen for early colonizers in teeth and implants, after 24 h of biofilm formation some similarities were found by 16S rDNA sequencing on Ti and enamel surface, with both surfaces colonized by Firmicutes, Proteobacteria, Fusobacteria, Bacteroidetes, Actinobacteria, and candidate division TM7 (Melo et al., 2017). In spite of the microbiome similarity in biofilms formed in teeth and implant surfaces in health, a cross-arch controlled *in vivo* study showed that smooth implant surfaces accumulated less biofilm than teeth and showed a more heterogeneous microbiome shift during the absence of oral hygiene, which promoted inflammation around both implants and teeth (Schincaglia et al., 2017). In fact, even

with some biogeographic proximity and similar oral microenvironment, dental and implant surfaces can show significant differences in their microbial ecosystems (Dabdoub et al., 2013). These differences may be explained by the higher clinical signs of inflammation at tooth sites compared with implants (Zitzmann et al., 2001; Schincaglia et al., 2017), which may modulate microbiome composition. Because surface properties such as chemical composition and roughness affect the first step of biofilm formation (Souza et al., 2020a), certain differences in microbial attachment are expected even in early stages. However, subsequent environmental pressures, such as local degree of inflammation, may further modulate the late stage of microbial community growth.

Relationship between bacterial microbiota and peri-implant tissue damage

Polymicrobial biofilms forming on dental implant surfaces are considered the main etiologic factor for inflammatory disease processes known as peri-implant mucositis and peri-implantitis (Berglundh et al., 2018). These conditions are the main reason for dental implant treatment failure showing a high prevalence, with more than 40% of implants affected by mucositis and more than 22% affected by peri-implantitis (Salvi et al., 2017). In the oral cavity, peri-implant mucositis is characterized by inflammation in the mucosa around dental implants, but its progression and subsequent progressive loss of supporting bone is known as peri-implantitis (Berglundh et al., 2018). Both conditions are considered as "biofilm-associated pathological conditions," and therefore, there is a strong evidence that biofilm is the main etiological factor for dental implant-related infections (Berglundh et al., 2018). In fact, biofilms have been described as physical and chemical "stress" factor triggering inflammatory processes on surrounding tissues (Marsh et al., 2011). Initial biofilm growth by early colonizers promotes the colonization and growth of more virulent late colonizers, which increase the overall pathogenicity of the biofilm. This pattern is often associated with an exacerbated inflammatory response followed by significant peri-implant mucosal damage and peri-implant bone resorption (Heitz-Mayfield and Lang, 2010; Nguyen et al., 2017).

Classic animal studies have used biofilm-retaining ligatures to prove cause-effect relation from increased biofilm accumulation and directly correlated this to worse clinical measures, such as bleeding, greater probing depth, loss of attachment, and reduced bone density in natural teeth and implanted devices (Lindhe et al., 1992; Lang et al., 1993; Schou et al., 1993). Interestingly, Schou et al. (1993) also showed that bone loss around implants was significantly greater than around teeth; the study therefore suggested that the presence of marginal inflammation around implants may have more serious clinical implications than does marginal inflammation around teeth with a periodontal ligament. More recently, clinical signs of disease progression were also linked to microbiological changes and transition to a more pathogenic biofilm on dental implant surfaces (Shibli et al., 2008; Padial-Molina et al., 2016). Remarkably, a niche specificity was also shown on dental implant disease sites, in which biofilm composition was different between supra- and sub-mucosal sites, with *Veilonella parvula* and certain *Streptococcus* species being more prevalent at supra-mucosal compared with sub-mucosal sites (Shibli et al., 2008). However, in both sites, there was a significantly higher proportion of putative pathogens and reduced abundance of beneficial species during peri-implant infection, when compared with healthy sites (Shibli et al., 2008). Despite some differences, the overall biofilm composition on dental implant surfaces during peri-implant infection still has major similarities with that associated with periodontal diseases. In fact, a systematic review showed that there is insufficient evidence to support specific differences in the microbiota (specific pathogens) between teeth and implants, either in health or in disease on late biofilm states (Retamal-Valdes et al., 2019). This is corroborated by microbiome studies showing a high level of similarity between the microbial profile of periodontitis and peri-implantitis, especially in species that are prevalent in late stages of biofilm formation during disease (Kumar et al., 2012). Interestingly, a similarity between healthy and diseased sites exists in the microbiota that is higher for peri-implant than periodontal diseases (Kumar et al., 2012), showing a strong effect of the implant surface in modulating the microbiome communities formed on its surface in health or disease. In peri-implant disease microbial communities show a lower diversity, compared with healthy sites, supporting a true dysbiotic state, in which lower levels of *Prevotella* and *Leptotrichia* and higher levels of *Actinomyces*, *Peptococcus*, *Campylobacter*, *nonmutans Streptococcus*, *Butyrivibrio*, and *Streptococcus mutans* were reported (Kumar et al., 2012). This is in contrast to periodontal diseases where the bacterial diversity in inflammation-associated biofilms is higher than health-associated biofilms (Abusleme et al., 2013).

Moreover, *in vivo* studies have shown higher total bacteria counts in peri-implantitis biofilms (where not only the smooth but also the rough treated surface of the implant is colonized by biofilm) compared

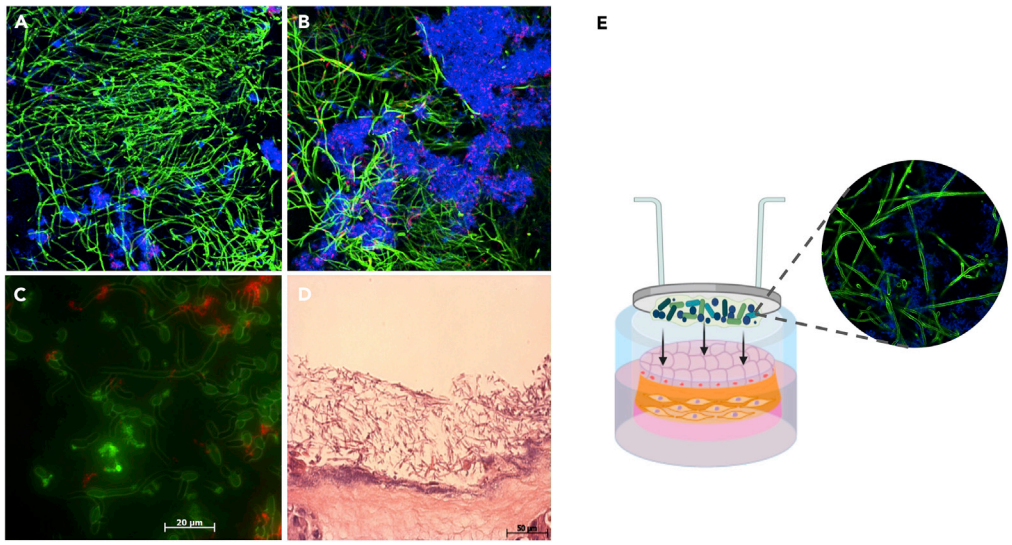

Figure 3. *Candida* and *Streptococcus* mixed-biofilms on titanium surface

(A and B) Twenty-four-hour mixed biofilm stained by immuno-FISH of *Candida albicans* (green) and *Streptococcus oralis* (stained in blue on A and B and in red on C) growing on (A) titanium surface and (B) polystyrene surface. Bacterial extracellular matrix is stained with Alexa Fluor 647-labeled dextran conjugate probe (red) in figure (B). Images suggest that biofilm growth is modulated by the type of surface.

(C) *C. albicans* (green) and *S. oralis* (red) interaction on biofilm growing on the polystyrene surface.

(D) Dual species biofilms growing on the organotypic mucosal construct, which can cause epithelial barrier breach (H&E stain).

(E) Titanium-mucosal interface biofilm model. Biofilm formed on titanium surface suspended 0.5 to 1 mm above the *in vitro* organotypic mucosal construct surface. Reprinted (adapted) from refs (Souza et al., 2020c, Souza et al., 2020d); Copyright (2020), with permission from American Society for Microbiology and Springer Nature. Figure E created by BioRender®.

with healthy sites (where only the smooth supra-mucosal implant surface is colonized by biofilms), with increased levels of *T. forsythia, T. denticola, F. nucleatum, P. intermedia, P. micros, C. rectus, E. corrodens, Candida albicans, P. nigrescens, C. gracilis, C. ochracea, C. concisus, Streptococcus spp., A. odontolyticus, V. parvula*, and *E. faecalis* (Canullo et al., 2017). Earlier studies also identified *T. forsythia* in higher abundance in sub-mucosal biofilm samples of peri-implantitis subjects (Shibli et al., 2008).

It is interesting to also highlight the increased presence of *C. albicans* in peri-implantitis biofilms. Although not frequently evaluated in human peri-implant disease studies, *C. albicans* can grow on Ti surfaces and has been clinically isolated from biofilms associated with peri-implant disease (Leonhardt et al., 1999; Schwarz et al., 2015; Canullo et al., 2017), possibly due to its ability to form robust mixed biofilms with *Streptococcus* species. Recently our group showed that *C. albicans*, an oral fungal opportunistic pathogen, increases tissue damage when growing in biofilms at the titanium-mucosal interface (Souza et al., 2020c). Using an *in vitro* titanium-mucosal interface model we showed that mixed biofilms of *C. albicans* and *Streptococcus* species have a mutualistic relationship, promoting bacterial growth and augmenting expression of *Candida* virulence genes (Souza et al., 2020c). Our studies also showed that cross-kingdom interactions between *C. albicans* and *S. oralis* are modulated by different substrates on which the biofilm is growing. *Candida* stimulates increased glucosyltransferase R expression, an enzyme responsible for the bacterial extracellular matrix, on Ti but not on plastic surfaces (Souza et al., 2020d). Similar mutualistic relationships between *C. albicans* and *Streptococcus* species have been described in biofilms growing directly on biotic (oral mucosa) and abiotic (i.e. plastic, titanium) surfaces (Xu et al., 2014a, 2014b; Souza et al., 2020c). These biofilms trigger an exacerbated inflammatory host response and increased tissue damage but have been explored mainly in the context of mucosal infection (Xu et al., 2014b; Bertolini et al., 2019). Although *Candida* forms biofilms on Ti surfaces (Figure 3), its role on peri-implantitis has not been adequately investigated. In fact, a complete microbiological profile of peri-implant infections including both bacteria and

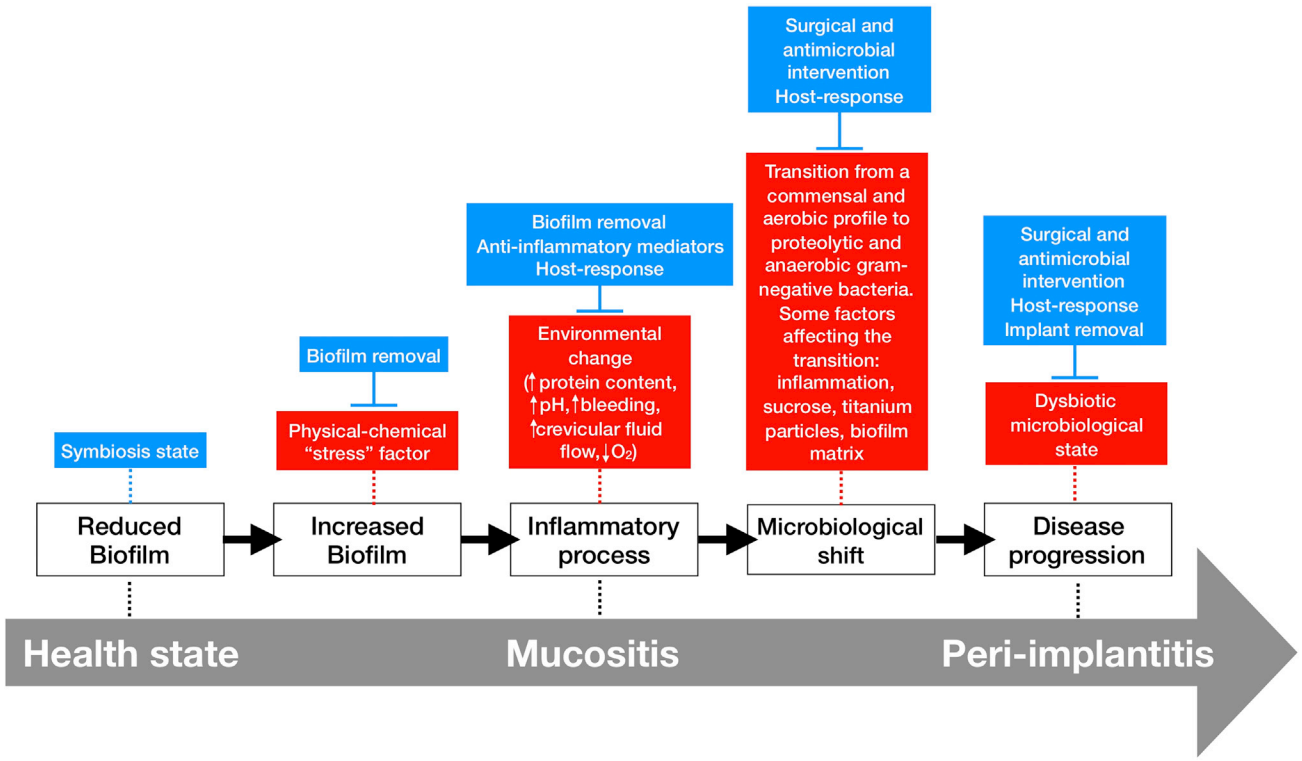

Figure 4. Schematic representation of the "ecological plaque hypothesis" in relation to peri-implant disease, adapted from Marsh et al. (2011) and Rosier et al. (2018)

Increased biofilm accumulation on implant surface triggers an inflammatory process that changes the environment leading to microbiological shift and disease progression, as shown by red boxes. Other factors can also favor the microbiological shift on biofilms growing on titanium surfaces, such as carbohydrate (sucrose exposure). However, some factors can control biofilm accumulation and inflammatory response, shown in blue boxes, such as surgical and antimicrobial intervention and host-response.

fungi at different stages of disease and their effect on soft and hard tissue damage need further investigation.

Factors affecting microbial diversity in oral biofilms

A symbiotic relationship may be established between a polymicrobial biofilm and the host as long as biofilm control methods are routinely applied to maintain low levels of microorganisms on implant surfaces (Schincaglia et al., 2017). However, when left undisturbed biofilms mature, and this may lead to increased inflammation and a rise in the crevicular fluid volume, which provides nutrients for further microbial growth and disruption of host homeostasis (Sultan et al., 2018; Rosier et al., 2018; Naginyte et al., 2019). An adaptation from the "ecological plaque hypothesis" on tooth surfaces may be applied to describe a transition from a healthy state to a disease state in the peri-implant mucosa and bone structures (Figure 4) (Marsh et al., 2011). According to this model, increased biofilm accumulation, mainly due to lack of adequate biofilm removal/disruption (oral hygiene procedures), acts as a "stress" factor triggering an inflammatory process that leads to changes in the local microenvironment, favoring proteolytic and anaerobic gram-negative bacterial overgrowth (Marsh et al., 2011). This inflammatory response may be limited to the peri-implant mucosa and is known as mucositis. A long-standing mucositis can contribute to a microbiological shift favoring disease progression to the alveolar bone leading to peri-implantitis. Alternatively, an anti-inflammatory cytokine feedback loop may control the local inflammatory process and prevent disease progression (Rosier et al., 2018). Although the transition from a healthy oral microbiome to a disease-associated microbiome on biomaterials is still not fully understood, some environmental factors that may contribute to a dysbiosis state in biofilms are carbohydrate exposure, Ti particles and ions released from the implant biomaterial, and presence and composition of an extracellular matrix (Jenkinson, 2011;

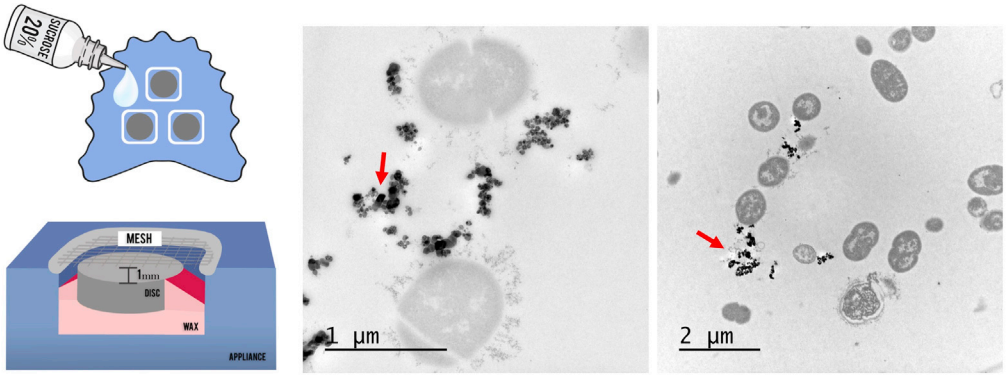

Figure 5. Schematic representation of the *in situ* model used to form biofilm on titanium surface using palatal appliances

Sucrose is used to promote biofilm accumulation and extracellular matrix formation. Transmission electron microscopy showing biofilms formed *in situ* on Ti surface and exposed to Ti particles treatment. Red arrows showing Ti particles agglomerated and precipitated Ti ions on extracellular sites. Reprinted (adapted) from Ref. (Souza et al., 2019a); Copyright (2020), with permission from John Wiley and Sons.

Bowen et al., 2018; Souza et al., 2019a, 2020e). Thus, even though the initial protein adsorption will mediate the primary and secondary colonizers during bacterial attachment, biofilm formation and maturation is a complex process determined not only by the surface properties, the host-response, and environmental conditions (Cheng et al., 2019).

Sucrose is a unique dietary carbohydrate as it is the only substrate leading to production of streptococcal glucans that constitute the main extracellular matrix component of dental biofilms (Xiao et al., 2012; Koo et al., 2013; Souza et al., 2020d) and promote increased biofilm accumulation on dental surfaces (Ccahuana-Vásquez et al., 2007). Our group recently showed that this carbohydrate can also favor biofilm growth on Ti surface, as evaluated *in situ* (Souza et al., 2019a). Moreover, increased biofilm accumulation and the ensuing microbial succession on Ti surfaces due to sucrose exposure (20%, four times/day) led to a microbial dysbiotic shift favoring anaerobic putative pathogens by day 7 (Souza et al., 2019a).

In addition to sucrose, recent work showed that Ti ions and particles commonly released by implants due to mechanical and chemical degradation processes (wear debris from the implant-abutment connection, stripping off from the implant surface while placing, or manipulations during peri-implant surface treatment, ions released from the corrosive environment—acidic pH, microbial accumulation, or chemical agents) also promote a dysbiotic pathogenic biofilm growth on Ti surface (Figure 5) (Souza et al., 2020e). Although Ti itself is not bacteriostatic, *in vitro* studies have shown a biocidal effect of metal and metal oxide nanoparticles (e.g., zinc oxide, copper oxide, nickel, titanium dioxide) (Yu, 2004; Khan et al., 2015). Nanoparticles cause direct disruption of bacterial cell membrane integrity, as well as induction of oxidative stress by free radical formation and possibly lead to protein and DNA damage (Khan et al., 2015). Because nanoparticle susceptibility and tolerance are species dependent, metal nanoparticles can alter the bacterial biofilm composition and cause a dysbiotic state that favors overgrowth of certain species (Souza et al., 2020e). Other factors that change the microenvironment and may affect the microbiological shift are the extracellular biofilm matrix components. Extracellular polymers in biofilm matrix are responsible for the biofilm three-dimensional architecture (Souza et al., 2020d), generating a highly concentrated nutrient availability and reduced O_2 levels (Xiao et al., 2012), which may create a suitable microenvironment for the growth of strict anaerobic putative pathogens. However, the specific effects of extracellular polymers for biofilms growing on Ti surface are still unknown and require further investigation.

Topography properties and current strategies to control polymicrobial biofilms on titanium surfaces

As mentioned earlier, biomaterial surface properties can modify microbial adhesion by selective adsorption of salivary and/or plasma proteins. Both physical and chemical properties of Ti material affect protein adsorption profile (Pantaroto et al., 2019; Souza et al., 2020a). Evidence has suggested that negatively charged surfaces, superhydrophobic and superhydrophilic surfaces, and nm-scale surface characteristics

can reduce initial microbial adhesion (Song et al., 2015). Thus, among physical-chemical modifications that have been proposed so far to alter Ti surface properties, the most important are surface-free energy, wettability, charge, and topography in order to limit microbial adhesion. Roughness has been the most evaluated surface property shown to affect microbial adhesion, and although moderate surface roughness may favor microbial adhesion due to a higher contact area between the surface and cells, increased adhesion does not occur on nm-scale or highly roughened surfaces (implant surface with Sa—arithmetical mean height—parameter of more than 2.0 μm) (Albrektsson and Wennerberg, 2004; Whitehead et al., 2006; Puckett et al., 2010; Song et al., 2015). Moreover, the distribution of peaks and valleys affect microbial adhesion directly, because topographic patterns with different shape and size have been shown to inhibit biofilm formation compared with flat surfaces (Song et al., 2015).

It is important to highlight that topographical patterns of titanium surfaces may play distinct roles in the dynamics of biofilm growth especially for surfaces with a nm-scale pattern (Puckett et al., 2010; Lorenzetti et al., 2015; Cao et al., 2018). For example, Cao et al. (2018) showed that the spear- and pocket-type nanostructures synthesized via hydrothermal treatment on Ti have shown different antimicrobial potential. The spear-type surface presented little space between the spears, and therefore, the bacteria are only able to position themselves at the tips of the nano-spears. This not only allows a low initial bacterial load but also causes membrane damage and perforations, leading to cell death. However, this anti-biofilm mechanism is unsustainable because the dead bacteria can cover the nano-spears, which would otherwise prevent killing of new arrivals, and allow the formation of a thick biofilm over a period of 6 days. In contrast, the more promising anti-biofilm effect of pocket-type nanostructure is associated with an open porous mesh structure of randomly oriented spears that permit bacterial localization inside the pockets. In this case, bacteria are killed either by direct membrane penetration or by severe membrane deformation. As the biofilm develops over time and the bacterial load increases, more cells accumulate in the inner voids, resulting in cell death by direct penetration/compression from the spears. As a result, only small clusters of live bacteria are identified on the rim of the pockets after 6 days. Importantly, when it comes to these two nanostructures, it seems that wettability properties do not appear to play an important role on anti-biofilm properties. At a nanoscale, surface topography (diameter of nano-spears and spacing between them) rather than surface roughness (spear height) may be the dominant factor in bacterial attachment and survival on the implant surface.

However, at micro-scale patterns, highly roughened surfaces (Sa > 2.0 μm) (Albrektsson and Wennerberg, 2004) have increased hydrophobicity, which can reduce initial bacterial adhesion. Interestingly, we showed that a superhydrophobic coating (Souza et al., 2020b) modified the salivary pellicle composition at the proteomic level, leading to differences in the biofilm bacterial composition as compared with control surfaces. In fact, a superhydrophobic profile on Ti surfaces was shown to not only reduce bacterial and fungal adhesion and biofilm accumulation but also change the composition of adhered micro-organisms favoring a more host-compatible or symbiotic profile (Souza et al., 2020b). Thus, we hypothesized that the anti-biofilm property of the superhydrophobic surface may be related to a direct reduction of microbial adhesion due to hydrophobicity and also by an indirect effect conferred by the specific protein coating composition.

Based on evidence that surface properties directly affect biofilm formation, modifications by means of surface treatments have been proposed to enhance biological responses. Some treatments, such as sand-blasted, large grit, and acid-etched (SLA) surface, are commonly available as commercial dental implants due to enhanced primary stability and optimized osseointegration process when compared with machined implants (Li et al., 2002). However, the increased surface roughness obtained by this type of treatment also favors biofilm accumulation if this surface becomes exposed in the oral cavity (Schmidlin et al., 2013). A promising strategy to control biofilm colonization is the development of surface coatings on Ti (Costa et al., 2020a). This approach has been developed using different technologies, such as glow discharge, electrolytic plasma, and photocatalytic materials, all resulting in bioactive surfaces with antibacterial properties (Ferraris and Spriano, 2016). Several antimicrobials, active molecules, compounds, and ions have been incorporated on Ti surface as biofilm-targeting approaches in order to reduce microbial attachment on the surface. Importantly, cell cytotoxicity and short-term efficiency are currently the main limitations of coatings developed so far for Ti surface (or Ti alloys) (Matos et al., 2017; Chang et al., 2018). Moreover, newly developed surface treatments or coatings should consider that bactericidal and/or bacteriostatic effect might not be enough to control biofilms in the long-term since dead cells remaining attached to the implant surface and can still act as binding sites for microorganism coaggregation, promoting colonization by live pathogens (Koo et al., 2017).

After a dysbiotic polymicrobial biofilm forms on implant surfaces leading to peri-implantitis, there is no consensus regarding the effective treatment for these infections (Heitz-Mayfield and Mombelli, 2014). Non-surgical and surgical therapies have been proposed to control or attempt to eradicate biofilm accumulated on implant surfaces to restore a state of peri-implant health (Heitz-Mayfield and Mombelli, 2014). Adjunct treatments using antimicrobial agents have been proposed in combination with mechanical debridement (Figuero et al., 2014). In fact, some locally delivered antimicrobial agents (such as citric acid, povidone iodine, chlorhexidine) have shown to be very effective on reducing viable bacteria on contaminated Ti surfaces by *in vitro* and *in situ* studies (Souza et al., 2018, 2019b).

Locally or systemically administered antibiotics have also been used as an adjunctive approach to mechanical therapy for peri-implant infections (Van Winkelhoff, 2012). Because they have shown only a moderate efficacy in the treatment of peri-implant infections, there is still no consensus regarding their application. Interestingly, the effect of systemic antibiotics in the treatment of severe cases of peri-implantitis may be enhanced by previous surface decontamination procedure, as shown by a clinical trial indicating that an improved outcome was found when systemic amoxicillin was used after the implant surface was debrided with the use of adjunct locally applied chlorhexidine agent (Carcuac et al., 2016). Other antibiotics such as doxycycline (Mercado et al., 2018) and minocycline (Renvert et al., 2006) have also showed a promising effect on implant-related infections. Interestingly, a clinical trial showed that the combination of amoxicillin and metronidazole, which is commonly used to treat periodontitis (Feres et al., 2015), did not show a significant effect in peri-implantitis management as adjunct with local mechanical debridement (Shibli et al., 2019). This result may be explained by a limited diffusion of antibiotics in biofilms forming within Ti surface irregularities and underscores the potential importance of surface topography. This supports the idea that slow release of drug-delivery surface coating methods may be more appropriate than systemic antibiotics in the treatment or prevention of peri-implantitis these infections.

Moreover, it is important to highlight that the anti-microbial effect of newly developed treatments should be evaluated mainly by *in vivo* models, because mucositis and peri-implantitis are chronic diseases and the host response can affect the growth and susceptibility of these biofilms, as well as the rate of drug delivery by surface coatings. Therefore, studies that evaluate only initial steps of microbial adhesion or initial biofilm formation may not show sustainable long-term results, which is an important aspect to consider in the chronic pathogenesis process *in vivo*. Although most treatments/coatings have been tested using mainly single-species biofilms, which may be useful for initial screening purposes, proper evaluations should take into account the diversity of the oral microbiome. In this regard, microcosm models using saliva or dental biofilm organisms as initial microbial inoculum or *in situ* models in the oral environment (Souza et al., 2018, 2019a) are more appropriate pre-clinical models. In addition, based on our current knowledge regarding the diversity and composition of health- and disease-associated biofilms, quantitative data regarding total bacterial loads are not sufficient to fully understand the effects of antimicrobials. The composition of biofilms in response to antimicrobials should also be evaluated using high-throughput methods such as DNA-DNA checkboard hybridization and metagenomics.

Emerging evidence for drug delivery coatings as a biofilm control strategy

More recently, controlled drug delivery systems have been proposed as coatings onto Ti surfaces (Fenton et al., 2018). These systems have certain advantages, such as controlled rate of release and the potential to use target-specific agents as surface coatings. However, antimicrobial surface coatings need to be developed considering characteristics such as (1) maintaining or enhancing the chemical, physical, and mechanical properties of the material; (2) non-cytotoxic effect to host tissues; (3) predictable long-term drug release; and (4) incorporation of proper drugs as target agents (Fenton et al., 2018). In this sense, dental implants covered by antimicrobial agents may act as a monolithic system, because the drug release is expected to be homogeneous over the entire surface (Pokrowiecki, 2018). This system must also provide an effective and stable drug concentration to avoid bacterial resistance on the peri-implant site (Pokrowiecki, 2018). However, because dental implants are expected to be functional for decades, the drug release coating needs to allow recharge/re-deposition when needed, or it may act only during initial healing process and initial biofilm formation. Although some drug delivery agents such as polylactide acid (PDLA) increase the release of drugs, the short-term release and inability to be reloaded are still the biggest limitations of this coating approach (Pokrowiecki, 2018).

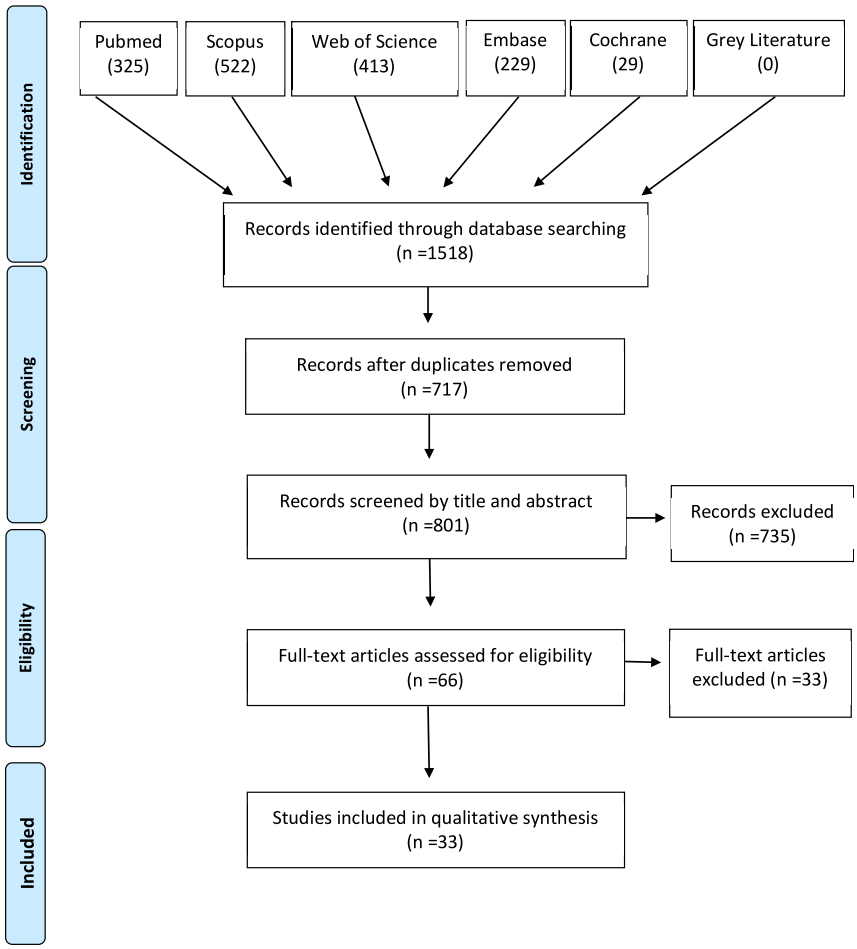

Figure 6. Diagram of the source and selection procedures, according to the PRISMA guidelines

A local drug delivery system composed of minocycline microspheres has shown some promising clinical results in treating peri-implant infections (Renvert et al., 2006), which has also been used in teeth with periodontal disease for more than two decades (Williams et al., 2001). However, more recent engineering approaches have provided modified materials for surface coating loaded with antibiotics as a new generation of biomaterials to control biofilm accumulation and, consequently, implant-related infections (Koo et al., 2017). The incorporation of antibiotics within a surface coating has been widely applied for Ti materials in the recent years (Nie et al., 2016; Zhang et al., 2019; Thompson et al., 2019). Although these coatings continue to be evaluated, their application *in vivo* has been challenging, due to short-term release characteristics, and possibly reduced release due to the protein layer adsorbed over the antibiotic coating, as well as cytotoxicity (Koo et al., 2017). Moreover, these treatments should consider surface topography properties to achieve an appropriate antimicrobial activity. In fact, currently there are no commercially available dental implants made of Ti loaded with antibiotics for clinical use. To the best of our knowledge there is no consensus regarding the optimal antibiotic and coating technique used on Ti material to achieve a reduced microbial load with the potential to control implant-related infections. In the following section we conduct a systematic review on this topic, which supports this conclusion.

RESULTS

Study selection

A diagram of the source and selection procedures, according to the PRISMA guidelines, is shown in Figure 6. The initial search identified a total of 1,518 references, including 325 in PubMed, 522 in Scopus, 413 in Web of Science, 229 in Embase, 29 in Cochrane, and 0 in Gray Literature. Of this total, 717 duplicates were removed, with 801 studies remaining. Title and abstract screening resulted in exclusion of 735 records

according to the eligibility criteria. The agreement between the two reviewers regarding the titles and abstracts selection was $\kappa = 0.73$. Consequently, 66 studies were selected for full-text reading. From that, 33 articles were excluded: two full text were not available (even after three attempts of contact with authors), six were excluded for other reasons (abstract, conference paper, and *in vitro* model) and 23 did not meet the eligibility criteria. Out of these 23 studies, 18 did not evaluate microbial colonization quantitatively on implant surface, four only evaluated microbial load in bone tissue surrounding the implant, two did not use Ti-based implants, and one human study was excluded due to the absence of a control group (references on Supplemental information). At this stage, the agreement between the two reviewers was $\kappa = 0.87$. A total of 33 records were included in the qualitative synthesis, and the main reason for each article exclusion was detailed in Supplemental information (Table S2, related to Figure 6). Importantly, based on our inclusion criteria no study with humans was included, with all studies using animal models.

Study characteristics

The implant and animal characteristics of the included studies are detailed in Table 1. All included articles were published between 2003 (Lucke et al., 2003) and 2020 (Auñón et al., 2020; Zeng et al., 2020), in twenty-four different countries. Among the implant materials, pure Ti, and titanium-aluminum-vanadium (Ti-Al-V), and titanium-aluminum-niobium (TiAlNb) alloys were used, and different surface treatments were evaluated. Anodized nanotubes and organic and biodegradable coatings were the most investigated surface treatments in association with the antibiotics. With regard to the antibiotic used, gentamicin (n = 11) and vancomycin (n = 11) were the most commonly tested, alone or combined, followed by rifampicin (n = 3), tobramycin (n = 2), doxycycline (n = 2), fosfomycin (n = 1), clindamycin (n = 1), teicoplanin (n = 1), ciprofloxacin (n = 1), minocycline (n = 1), enoxacin (n = 1), bacitracin (n = 1), and daptomycin (n = 1), as shown in Figure 7. Different technologies of deposition such as sol-gel, covalent immobilization, spraying, electrophoretic, polyelectrolyte, and dip coating were applied for antibiotic loading on the Ti surface. All retrieved papers adopted the *in vivo* design using different animal models (rats: n = 15, rabbits: n = 13, mice: n = 5). Implants were commonly located in tibia or femur. With regard to the infection model, *Staphylococcus aureus* was the most used (31 studies) with a wide range in bacterial inoculum size (102–109 CFU). *P. aeruginosa* (Badar et al., 2015) and *C. albicans* associated with *S. aureus* (Kucharíková et al., 2016) were also used as microbial inoculum. In addition, the effects of antibiotic-loaded coatings were evaluated in a broad range of follow-ups, varying from 4 h up to 1 month after implant inoculation at different time points. The long-term effect of antibiotic-loaded coatings was analyzed based on the longest follow-up time in each study.

Antibiotic-loaded coatings reduced microbial load on Ti-implants

The microbiological assessments of the included studies are detailed in Table 2. Among the quantitative tests for biofilm analysis, the viability of bacterial cells is reported by colony count units (CFU) after implant sonication and agar plating or rolling out the contaminated implant directly on agar plates. Overall, quantitative results on bacterial loads showed greater bacterial implant surface contamination in the control groups (i.e. machined surface or coating without antibiotic). In this systematic review we used the bacterial load (control and test groups) to calculate the percentage of biofilm reduction on antibiotic-loaded surfaces in each study. In addition, the long-term effect of biofilm reduction of antibiotic-loaded coatings was analyzed taking into account the longest follow-up time for each study. Based on this we found a highly variable % of biofilm reduction in different studies, ranging from 0% to >90% reduction (Figure 8). For gentamicin-loaded coatings, the reduction showed a variation of ~5% (Moskowitz et al., 2010) up to ~99.9% (Thompson et al., 2019), whereas for vancomycin-loaded coatings minimum and maximum values were ~45.3% (Kucharíková et al., 2016) and ~99.2% (Stavrakis et al., 2019), respectively. In contrast, three studies showed higher bacterial load on the test group as well as the absence of reduction with vancomycin (Ghimire et al., 2019), doxycycline (Metsemakers et al., 2015), or gentamicin (Neut et al., 2015) coatings. In addition, the infection rates (presence of contaminated implants) also were commonly smaller in test groups in terms of bacterial counts on agar plates when compared with control groups (Table 2). However, a long-term antibiotic release is not expected, because several studies showed more than 50% of released drugs taking place within hours or days (Lucke et al., 2005; Darouiche et al., 2007; Neut et al., 2015; Yuan et al., 2018; Thompson et al., 2019) (Table 2), with some treatments even showing more than 95% of the deposited drug released within short time periods (Neut et al., 2015; Ghimire et al., 2019; Thompson et al., 2019).

Table 1. Summary of included studies

	Implant				Animal				
Author	Material	Surface treatment	Antibiotics	Deposition technology	Type	N*	Surgical site	Infection model	Follow-up
Adams et al. (2009)	Ti6Al4V	Anodized	Vancomycin	Sol-gel	Rat	11	F	*S. aureus* (NR strain origin)	1, 2, 3, 4w
Alt et al. (2014)	Ti6Al4V	Machined	Rifampicin + Fosfomycin	Ink-jet	Rab	22 (11 MSSA+ 11 MRSA)	T	*S. aureus* (MSSA EDCC5055) (MRSA T6625930)	4w
Antoci et al. (2007)	Ti6Al4V	Machined	Vancomycin	Covalently link	Rat	9	F	*S. aureus* (ATCC 25923)	1, 2, 3w
Auñón et al. (2020)	Ti6Al4V	TiO_2 nanotubes	Gentamicin + Vancomycin	Drug adsorption	Rab	20	F	*S. aureus* (Human Sa5)	4w
Aykut et al. (2010)	cpTi	Si-sandblasted	Clindamycin or Teicoplanin	Spraying	Rab	30	T	*S. aureus* (ATCC 29123)	1w
Badar et al. (2015)	Ti6Al4V	Porous	Ciprofloxacin	Layered double hydroxides suspension	Mic	12	S	*P. aeruginosa* (PAO1 CTX::lux)	4h
Croes et al. (2018)	cpTi	Porous Porous + CS	Vancomycin	Electrophoretic deposition	Rat	18	T	*S. aureus* (ATCC 49230)	4w
Darouiche et al. (2007)	Ti6Al4V	Si-sandblasted	Minocycline + Rifampin	Spraying	Rab	25	F	*S. aureus* (P1 – variation of ATCC 25923)	1w
Diefenbeck et al. (2016)	Ti6Al4V	Plasmachemical oxidation	Gentamicin	Immobilization (TA or SDS)	Rat	15	T	*S. aureus* (ATCC 49230)	4w
Ghimire et al. (2019)	Ti6Al4V	Dopamine methacrylate + PEGDMA-Oligo HYD	Vancomycin	Covalently bond	Mic	22	F	*S. aureus* (Xen 29)	3w
Grohmann et al. (2019)	cpTi	Sandblasted and etched	Gentamicin	Polyelectrolyte adsorption (PEM + + PGA/HEP)	Rat	30	T	*S. aureus* (ATCC 49230)	4w
Janson et al. (2019)	cpTi	Anodization + alkaly treatment + HA	Tobramycin	Soaking method	Rab	5	F	*S. aureus* (ATCC 6538)	9d
Jennings et al. (2016)	cpTi	Machined	Vancomycin	Manual application (PH)	Rab	9	R	*S. aureus* (UAMS-1 strain)	1w
Kälicke et al. (2006)	cpTi	PLLA	Rifampicin + Fusidic acid	Solvent-casting	Rab	36	T	*S. aureus* (V 8189-94)	4w
Kucharíková et al. (2016)	cpTi	Beadblasted and etched	Vancomycin	Covalent immobilization	Mic	NR	S	*S. aureus* (SH1000) *C. albicans* (SC5314)	2d (fungal) 4d (bacterial)
Liu et al. (2017)	cpTi	Machined and nanotubular anodized surface	Gentamicin	Soaking method	Rab	36	T	*S. aureus* (ATCC 25923)	6w
Lucke et al. (2003)	cpTi	PDLLA	Gentamicin	NR	Rat	30	T	*S. aureus* (ATCC 49230)	6w
Lucke et al. (2005)	cpTi	Machined or PDLLA	Gentamicin	PDLLA suspension	Rat	30	T	*S. aureus* (ATCC 49230)	6w

(*Continued on next page*)

Table 1. *Continued*

	Implant				Animal				
Author	Material	Surface treatment	Antibiotics	Deposition technology	Type	N*	Surgical site	Infection model	Follow-up
Ma et al. (2017)	cpTi	Machined + NIR light	Gentamicin	Vacuum drying process onto PEG-MoS_2 coating + CS	Rat	18	S	*S. aureus* (NR strain origin)	1d, 3d, 1w
Metsemakers et al. (2015)	cpTi	Anodized + PLEX	Doxycycline	Spraying	Rab	28 (12 MSSA + 16 MRSA)	H	*S. aureus* MSSA (JAR60131) *S. aureus* MRSA (LUH15101)	4w
Moskowitz et al. (2010)	cpTi	Layer-by-layer	Gentamicin	Polyelectrolyte deposition	Rab	27	F	*S. aureus* (ATCC 49230)	4d, 1w
Neut et al. (2015)	Ti6Al4V	Al-blasted + HA	Gentamicin	Spraying + PLGA	Rab	14	F	*S. aureus* (ATCC 25923)	2d, 1w
Nie et al. (2016)	Ti6Al4V	Machined	Enoxacin	Covalent immobilization	Rat	24	F	*S. aureus* (ATCC 43300)	3w
Nie et al. (2017)	Ti6Al4V	Machined	Bacitracin	Immobilization	Rat	10	F	*S. aureus* (ATCC 25923)	3w
Song et al. (2017)	cpTi	Nanofiber	Doxycycline	Coaxial electrospinning	Rat	48	T	*S. aureus* (ATCC 49230)	4, 8, 16w
Stavrakis et al. (2019)	cpTi	PEG-PPS	Vancomycin or Tigecycline	Encapsulation in PEG-PPS solution	Mic	18	F	*S. aureus* (Xen36)	6w
Thompson et al. (2019)	TiAlNb	Ca-P	Gentamicin	Dip coating	Rat	18	T	*S. aureus* (JAR060131)	1w
Yang et al. (2016)	cpTi	Nanotubes	Gentamicin	Lyophilization + Vacuum-drying	Rat	9	F	*S. aureus* (ATCC 25923)	6w
Yuan et al. (2018)	cpTi	Machined	Vancomycin	Soaking method on nanotubes coating + catechol functionalization	Rat	6	F	*S. aureus* (ATCC 25923)	4w
Zeng et al. (2020)	cpTi	Machined +NIR light	Daptomycin	Immobilization with IR820 dye on PDA nanocoating	Rat	NR	T	*S. aureus* (ATCC 25923)	2w
Zhang et al. (2018)	Ti6Al4V	Plasma-sprayed	Vancomycin	Impregnated on the plasma-sprayed coating	Rab	20	T	*S. aureus* MRSA (ATCC 43300)	6w
Zhang et al. (2019)	Ti6Al4V	Machined	Vancomycin	Covalently bond	Mic	14	F	*S. aureus* (Xen29)	3w
Zhou et al. (2017)	Ti6Al4V	PDLLA	Tobramycin	Impregnated on PDLLA coating	Rab	12	T	*S. aureus* (ATCC 25923)	8w

Implants and animals data from included experimental studies (author, year; implant: material, surface treatment, antibiotics, deposition technology of the antibiotic; animal: type, sample number, surgical site, infection model; follow-up).

Notes: Implant surface treatment (TiO_2, titanium dioxide; Si,Silica; CS, chitosan; PEGDMA, polyethylene glycol dimethacrylate; Oligo, oligonucleotide; HYD, hydrogel; HA, hydroxyapatite; PLLA, poly-L-Lactide; PDLLA, poly(D,L-lactide); NIR, near-infrared light; PLEX, polymer-lipid encapsulation matrix; Al, aluminum; PEG, poly(ethylene glycol); PPS, poly(propylene sulfide); Ca-P, calcium and phosphorus). Deposition technology (TA, tannic acid; SDS, sodium dodecyl sulfate; PEM, polyelectrolyte multilayer; PL, polycation; PGA, polyanion; HEP, heparin; PH, phosphatidylcholine; NR, not reported; PDLLA, poly(D,L-lactide); PEG, polyethylene glycol; MoS2, molybdenum disulfide; CS, chitosan; PLGA, poly(lactic-co-glycolic acid); PPS, poly(propylene sulfide); PDA, polydopamine); Animals (Rat, rats; Mic, mices; Rab, rabbits), Sample number (N) (MRSA, methicillin-resistant *Staphylococcus aureus*; MSSA, methicillin-sensitive *Staphylococcus aureus*; NR, not reported), Surgical site (T, tibia; F, femur; S, subcutaneous; H, humerus; R, radius), Follow-up (h, hour; d, day; w, week). *Sample number reported is the total number of infected animals used for microbiological assessments of non-loaded and antibiotic-loaded surfaces.

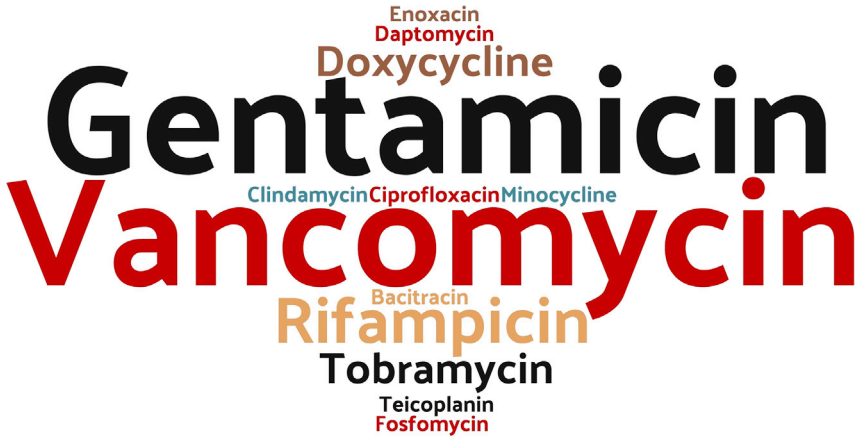

Figure 7. Word clouds of the antibiotics used on titanium coating in the studies included

The font size represents the frequency of antibiotics used in which bigger words mean more frequent antibiotics used.

DISCUSSION

Biofilms provide several advantages to colonizing species such as protection against host defense mechanisms, enhanced microbial co-aggregation, and reduced antimicrobial susceptibility (Costerton et al., 1995; Flemming and Wingender, 2010). These properties enhance microbial accumulation and maturation, which can trigger peri-implant infections. There is currently no consensus regarding the best therapeutic approach to treat dysbiotic biofilms and allow re-establishment of a health-associated microbiome. Newly developed strategies have been focused mainly on surface properties dedicated to non-fouling abilities and incorporation of antibiotics/antimicrobials on the surface as a long-term drug delivery method (Figure 9). Although this seems a promising strategy, no human clinical data are available regarding the efficacy of antibiotic-loaded implants in reducing microbial loads, as shown by our systematic review.

Although several studies included in this systematic review showed that the biofilms forming on antibiotic-loaded implants were considerably reduced (up to $\geq$90% biofilm reduction), a large discrepancy was found among studies testing the same antibiotic (Badar et al., 2015). This discrepancy can be ascribed to differences in study design and variable sample sizes that were not supported by power calculations. Badar et al. (2015) was the only study to perform implant placement before infecting the animals and to evaluate the antibacterial efficacy by measuring bacterial luminescence only 4 h after infection with *P. aeruginosa*. Moreover, the follow-up periods that studies reported were variable, and this may affect outcomes due to variable drug release kinetics.

In studies using the same antibiotic (gentamicin) and same bacterial species for inoculation (*S. aureus*), one methodology that provided lower values of biofilm reduction was when implants were rolled out on agar plates to quantitatively assess biofilm growth. Although this method is suitable to assess presence or absence of bacteria on the implant surface, it may not be sensitive enough to detect quantitative differences in bacterial loads (Lucke et al., 2003; Moskowitz et al., 2010; Liu et al., 2017; Grohmann et al., 2019). Studies that used a biofilm sonication step prior to plating, instead of the roll over agar method, were able to show a much greater biofilm reduction with antibiotic coating (Yang et al., 2016; Thompson et al., 2019). Sonication is a well-known technique to dislodge biofilms from the substrate and has been validated for the diagnosis of orthopedic implant prosthetic joint infections (Oliva et al., 2016). However, it is important to emphasize that different Ti surface treatments and antibiotic concentrations could also have influenced these differences in results.

In terms of the infection model, the choice of the appropriate microorganism is one of the most essential steps when evaluating biomaterials in implant-biofilm-related infections. With the exception of one study (Badar et al., 2015), the only experimental pathogen in the studies included in this review was *S. aureus*.

Table 2. Summary of microbiological data from included experimental studies (author, year; in vitro: drug concentration in the surface, drug release (related immersion period); microbiological assessments: quantitative test, mean and median of bacterial load (standard deviance); % reduction by authors calculated; infection rate; statistical significance)

	In vitro		Microbiological assessments					
				Bacterial load				
Author	Drug concentration in the surface	Drug release (immersion period)	Quantitative test	Control	Experimental	% Reduction	Infection rate	p value
Adams et al. (2009)	23.5 μg	70% (6 d)	CFU/implant + Rolled out on agar plates test (Infection rate)	1w: 11,230.67 (±299.5) 2w: 2,186.33 (±204.2) 3w: 17,7891.0 (±27,220.1) 4w: 18,765.0 (±4,493.75)	1w: 3.00 (±1.27) 2w: 1.57 (±0.57) 3w: 12,989.0 (±822.07) 4w: 4,531.5 (±221.2)	~75.8%	NR	NR
Alt et al. (2014)	307 μg rifampicin and 1,522 μg fosfomycin	NR	Rolled out on agar plates test	NR	NR	NR	C: 100% (5/5) T: 16.7% (1/6)	0.015
Antoci et al. (2007)	NR	NR	CFU/implant	1w:1,43,814.43 (±10,051.54) 2w: 87,951.81 (±7,831.33) 3w: 22,6315.79 (±11,403.51)	1w: 10,458.17 (±1,494.02) 2w: 25,903.61 (±1,807.23) 3w: 1,33,333.33 (±14,912.28)	~58.9%	NR	0.046 (1-w follow-up)
Auñón et al. (2020)	1.45 mg of gentamicin and 1.4 mg of vancomycin	56% gentamicin and 10.66% vancomycin (240 min)	CFU/cm^2 (Log_{10})	1.52 (±1.5)	0.15 (±0.47)	~90.1%	NR	0.0074
Aykut et al. (2010)	NR	NR	Positive or negative culture	NR	NR	NR	C: 100% (10/10) TEI: 0% (0/10) CLIN: 10% (1/10)	<.001 (C versus TEI, and C versus CLIN)
Badar et al. (2015)	1.2 mg/cm^2	NP	Bioluminescence intensity	1w: 100.56 (±28.4) 2w: 99.40 (±37.64) 3w: 289.88 (±21.30)	1w: 26.47 (±4.67) 2w: 68.45 (±28.03) 3w: 276.19 (±47.43)	~4.4%	NR	NR
Croes et al. (2018)	NR	NR	CFU/implant (Log_{10})	Uncoated: 5.01 (NR) CS control: 5.87 (NR)	5.63 (NR)	~4.4% (no difference)	C: 40% (2/5) CS control: 100% (8/8) T: 40% (2/5)	0.035 (CS control versus T for infection rate)

(*Continued on next page*)

Table 2. *Continued*

	In vitro		Microbiological assessments					
				Bacterial load				
Author	Drug concentration in the surface	Drug release (immersion period)	Quantitative test	Control	Experimental	% Reduction	Infection rate	p value
Darouiche et al. (2007)	35 μg/cm^2 (noncovalently bound)	94% minocycline and 95% rifampin (6 h)	Positive or negative culture	NR	NR	NR	C: 100% (12/12) T: 38.46% (5/13)	0.0016
Diefenbeck et al. (2016)	0.59 mg of G-SDS and 1.11 mg of G-TA	54.2 μg and 424.9 μg G from G-SDS and G-TA, respectively. (24 h)	Positive or negative culture	NR	NR	NR	C: 100% (10/10) G-SDS: 0% (0/10) G-TA: 10% (1/10)	NR
Ghimire et al. (2019)	90 μg/mm^3 hydrogel	~100% (24 h)	CFU/implant	3w: 520.0 (±40.0)	3w: 0	100%	NR	≤.01
Grohmann et al. (2019)	(PL-PGA)-20G = 0.32 (PL-PGA)-30G = 0.45 (PL-HEP)-20G = 0.15 (PL-HEP)-30G = 0.51 Data presented as referenced loads	(PL-PGA)-20G = 5.52 μg/cm^2 (PL-PGA)-30G = 18.62 μg/cm^2 (PL-HEP)-20G = 46.89 μg/cm^2 (PL-HEP)-30G = 86.21 μg/cm^2 (14 d)	CFU/implant (1/mm^2) (rolled over agar)	19.17*	(PL-PGA)-20G = 3.33* (PL-PGA)-30G = 12.50* (PL-HEP)-20G = 19.17* (PL-HEP)-30G = 3.33*	(PL-PGA)-20G = ~83.1% (PL-PGA)-30G = ~34.8% (PL-HEP)-20G = ~0% (PL-HEP)-30G = ~82.7%	NR	NR (No difference)
Janson et al. (2019)	NR	758 μg (15 min)	CFU/implant	(BC-10^4): 3.43 (±2)×10^5 (BC-10^5): 2.85 (±1.4)×10^5	(BC-10^4): 0.48×10^5 (BC-10^5): 0	(BC-10^4): ~85.9% (BC-10^5): 100%	C (BC-10^4): 100% (3/3) C (BC-10^5): 100% (2/2) T (BC-10^4): 33% (1/3) T (BC-10^5): 0% (0/2)	NR
Jennings et al. (2016)	25%	NR	CFU/implant	600,000 (NR)	20 (±21)	~99.9%	NR	<.001
Kälicke et al. (2006)	3% Rifampicin and 7% fusidic acid	~80% (42 d)	Harvesting	NR	NR	NR	C: 83% (10/12) PLLA-C: 83%(10/12) T: 17% (2/12)	0.033 (controls versus test)
Kucharíková et al. (2016)	35 pmol/cm^2	NR	CFU/implant (Log_{10})	*S. aureus*: 5.37 (±0.41) *C. albicans*: 4.47 (±0.15)	*S. aureus*: 2.92 (±0.25) *C. albicans*: 3.00 (±0.24)	*S. aureus*: ~45.6% *C. albicans*: ~32.9%	NR	<.05 (*S. aureus*) NR (*C. albicans*)
Liu et al. (2017)	NR	NR	Rolled out on agar plates test	Ti-C: >1000 CFU NTATi-C: >1000 CFU	Ti-G: 473.75 (±10.69) NTATi-G: 40.5 (±12.36)	Ti-G: ~52.6% NTATi-G: ~95.9%	C: 100% (4/4) NTATi-C: 100% (4/4) Ti-G: 100% (4/4) NTATi-G: 100% (4/4)	<.05

(*Continued on next page*)

Table 2. *Continued*

Author	*In vitro*		Microbiological assessments					
	Drug concentration in the surface	Drug release (immersion period)	Quantitative test	Bacterial load		% Reduction	Infection rate	p value
				Control	Experimental			
Lucke et al. (2003)	10%	NR	Rolled out on agar plates test	Ti-C: >1,000 CFU PDLLA-C: >1,000 CFU	182 (±101)	~81.8%	Ti-C: 100% (10/10) PDLLA-C: 100% (10/10) T: 70% (7/10)	<.05
Lucke et al. (2005)	10%	60% (24 h)	Rolled out on agar plates test	Ti-C: >1,000 CFU PDLLA-C: >1,000 CFU	NR (range 7–136 colonies)	NR	Ti-C: 100% (10/10) PDLLA-C: 100% (10/10) T: 10% (1/10)	NR
Ma et al. (2017)	NR	- NIR: 2.8 mg/mL + NIR: 6.5 mg/mL (25 min)	Antibacterial ratio (%)	1d – Ti + NIR: 0.92% (±7.32) 3d – Ti + NIR: 82.42% (±2.75) 1w – Ti + NIR: 88.22% (±4.58) 1d – Ti – NIR: 0% (±6.14) 3d – Ti - NIR: 70% (±4.91) 1w – Ti – NIR: 81.05% (±3.68)	1d – T + NIR: 99.15% (±1.83) 3d – T + NIR: 99.67% (±0.91) 1w – T + NIR: 99.97% (±0.91) 1d – T – NIR: 60.75% (±4.91) 3d – T – NIR: 88.59% (±2.45) 1w – T – NIR: 99.42% (±1.23)	NR	NR	<.001 (1d and 3d for + NIR; 1d for –NIR); <.01 (7d for –NIR); <.05(1w + NIR; 3d for –NIR)
Metsemakers et al. (2015)	3.4 mg	~95% (4 w)	CFU/implant (Log_{10})	MSSA: 5.10* MRSA: 4.89*	MSSA: 0* MRSA: 0*	At least 3-log lower median numbers of CFUs (no significant difference)	MSSA - C: 80% (4/5) MSSA - T: 0% (0/6) MRSA - C: 100% (8/8) MRSA - T: 43% (3/7)	<.05 (infection rate)
Moskowitz et al. (2010)	550 μg/cm^2	~100% (5.5 w)	Rolled out on agar plates test	4d: >200 CFU 1w: >200 CFU	4d: <22 CFU 1w: <190 CFU	4d: ~89.0% 1w: ~5.0%	4d - C: 83% (5/6) 4d - T: 0% (0/6) 7d - C: 71% (5/7) 7d - T: 0% (0/8)	NR
Neut et al. (2015)	1 mg/cm^2	~100% (168 h)	CFU/implant (Log_{10})	2d: 4.82 (±1.32) 1w: 3.60 (±2.64)	2d: 0 1w: 0	100%	C: 100% (7/7) T: 0% (0/7)	0.001
Nie et al. (2016)	NR	"*the covalent modification of the Ti surfaces does not allow the release of any antibiotic*"	CFU/implant (Log_{10})	6.20 (±0.18)	4.56 (±0.16)	~26.5%	NR	<.05

(*Continued on next page*)

Table 2. *Continued*

Author	*In vitro*		Microbiological assessments					
	Drug concentration in the surface	Drug release (immersion period)	Quantitative test	Bacterial load		% Reduction	Infection rate	p value
				Control	Experimental			
Nie et al. (2017)	NR	NR	CFU/implant (Log_{10})	4.67 (±2.34)×10^5	3.3 (1.67)×10^3	~99.3%	NR	<.05
Song et al. (2017)	NR	NR	Washout of implants (O.D. values)	4w: 0.17 (±0.24) 8w: 0.29 (±0.30) 16w: 0.64 (±0.06)	4w: 0.04 (±0.02) 8w: 0.04 (±0.01) 16w: 0.29 (±0.29)	~54.7%	8w - C: 100% (5/5) 8w - T: 0% (0/5) 16w - C: 100% (5/5) 16w - T: 40% (2/5)	<.005
Stavrakis et al. (2019)	NR	~23μg vancomycin (1 w)	CFU/implant (Log_{10})	2.8 (±1.5)×10^2	Vanco: 2 (±2) Tig: 1.8 (±1.8)×10^1	Vanco: ~99.3% Tig: ~93.6%	NR	NR
Thompson et al. (2019)	311.32 μg/mL	>95% (15 min)	CFU/implant (Log_{10})	1.76×10^6 (NR)	6.43 ×10^1 (NR)	~99.9%	C: 100% (9/9) T: 12.5% (1/8)	<.01
Yang et al. (2016)	NR	91.45 μg (57 h)	CFU/implant	Ti-C: 6.7×10^5 (±7.55×10^4) NT-C: 4.6×10^5 (±6.24×10^4)	1.57×10^4 (±2.08×10^3)	NT: ~97.7% T: ~96.6%	NR	<.01
Yuan et al. (2018)	NR	81.7% (24 h in the presence of *S. aureus*)	CFU/implant (Log_{10})	3.43 (±0.12)	0.90 (±0.43)	~73.8%	NR	<.01
Zeng et al. (2020)	634.6 μg	408.3 μg (14 d)	CFU/implant	Ti-C - NIR: 192.5 (±12.5) Ti-C + NIR: 182.5 (±22.5)	T - NIR: 82.5 (±10.0) T + NIR: 5.00 (±2.5)	NIR^-: ~57.1% NIR^+: ~97.3%	NR	<.01 (Ti-C versus T) <.05 (T - NIR versus T + NIR)
Zhang et al. (2018)	NR	NR	CFU/implant	8.42 (±0.68)×10^5	4.04 (±0.89)×10^4	~95.2%	NR	<.05
Zhang et al. (2019)	NR	NR	CFU/implant	1,478.26 (±521.74)	65.22 (±65.21)	~95.6%	NR	<.05
Zhou et al. (2017)	25% (4 mg)	26.03 ng/mL (released in the blood after 2 h implant installation)	CFU/implant	>10^4	<10^3	~90.0%	C: 100% (6/6) T: 16.7% (1/6)	<.05 (infection rate)

Notes: In vitro (NR, not reported; NP, not possible to extract data from the graph; G, gentamicin; SDS, sodium dodecyl sulfate; TA, tannic acid; PL, polycation; PGA, polyanion; HEP, heparin; d, days; min, minutes; h, hours; w, weeks); Quantitative test (CFU, colony forming unit; O.D., optical density); Microbiological assessments (NR, not reported; d, day; w, week; CS, chitosan; * = median; PL, polycation; PGA, polyanion; HEP, heparin; G, gentamicin; BC, bacterial concentration; CFU, colony forming unit; Ti, titanium; C, control group; NTA, nanotubular anodized surface; PDLLA, poly(D,L-lactide); +NIR, with near-infrared light; −NIR, without near-infrared light; T, test group; MRSA, methicillin-resistant *Staphylococcus aureus*; MSSA, methicillin-sensitive *Staphylococcus aureus*; Vanco, vancomycin; Tig, tigecycline; NT, nanotubes); Infection ratio (NR, not reported; C, control group; T, test group; TEI,teicoplanin; CLIN, clindamycin; CS, chitosan; G, gentamicin; SDS, sodium dodecyl sulfate; TA, tannic acid; BC, bacterial concentration; PLLA, poly-L-lactide; Ti, titanium; C, control group; NTA, nanotubular anodized surface; PDLLA, poly(D,L-lactide); MRSA, methicillin-resistant *Staphylococcus aureus*; MSSA, methicillin.

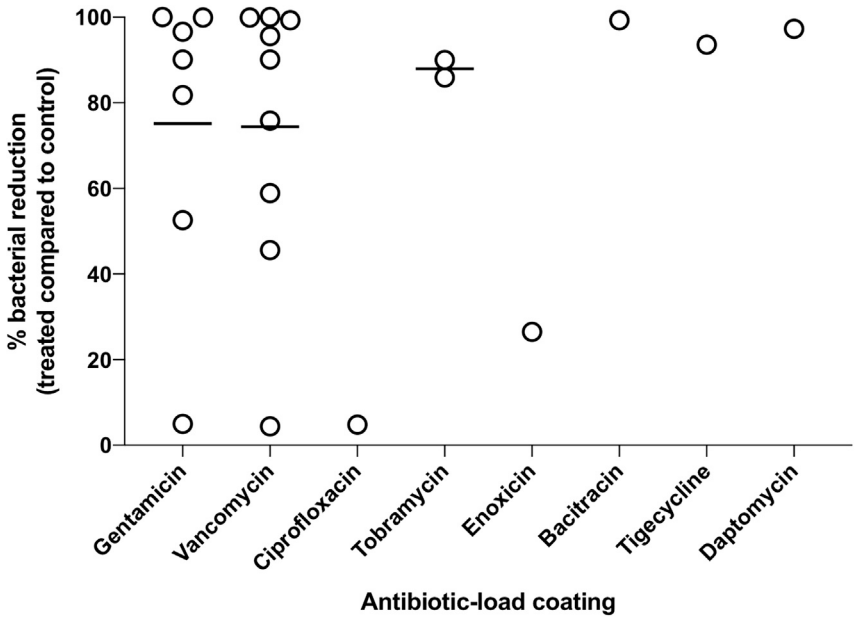

Figure 8. Percentage of reduction in the bacterial load on different antibiotic-loaded coatings on titanium surface in relation to control groups according to the study results included in this systematic review

Circles represent each study included in the review in which it was possible to calculate bacterial load reduction and to compare studies using the same antibiotic coating.

Although *S. aureus* is highly associated with postoperative infection in orthopedic implants (Oliveira et al., 2018), these results should be interpreted with caution since the presence of other microorganisms in the peri-implant microbiome was not evaluated. In addition, implants were commonly installed in tibia or femur sites, which do not widely represent the environmental conditions and healing of the oral cavity. Thus, the use of a polymicrobial infection model developed in the oral environment could provide more clinically relevant information regarding the effect of antibiotic-loaded coatings in reducing the microbial load. Surprisingly, biofilm-retaining ligature models to study oral multi-species biofilm accumulation on dental implant surfaces loaded with antibiotics are non-existent.

Early microbial colonization may occur during the surgical procedure of implant placement, often associated with immediate pathogen attachment on the implant surface through the surgical site (Hickok and Shapiro, 2012). Therefore, biofilm formation could start during the early stages of post-operative healing and may compromise the osseointegration process (Franz et al., 2011). Thus, drug delivery systems via surface coating may act as effective prevention methods to control microbial accumulation at the time of implant placement (Hickok and Shapiro, 2012). From the studies reporting the quantification of antibiotic release included in our systematic review, approximately 95% of the deposited drug was released within hours or days. Such early, rapid release would allow biofilm prevention in the immediate postoperative window but would not address the chronic peri-implant infection (Salvi et al., 2017; Berglundh et al., 2018), unless the antibiotic coating allows slower drug release so that its effect lasts for a longer period of time. The literature has pointed out that the use of layer by layer assembly might be the most advantageous and intelligent releasing system for long-term release, as the drug is entrapped between layers and is sustained eluted through film-erosion and/or diffusion (Smith et al., 2009; Perni et al., 2020). Further advantage of this system is that the layer can be programmed to degrade under acidic conditions (e.g. infection with aciduric species), such that the drug is available only when necessary. Ultimately, the efficacy of an antibiotic releasing system combined with surface topographic modification approaches (e.g. pocket-type nanostructure Ti surfaces) (Cao et al., 2018) deserves further investigation for implant applications. Experimental work using different bacterial species are required to test the effectiveness of the developed nanostructured surfaces in addition to mechanical tests evaluating structural stability under attrition (during bone insertion and torque). *In vivo* testing in appropriate animal models (e.g. oral biofilm ligature models) will also need to be conducted in the future.

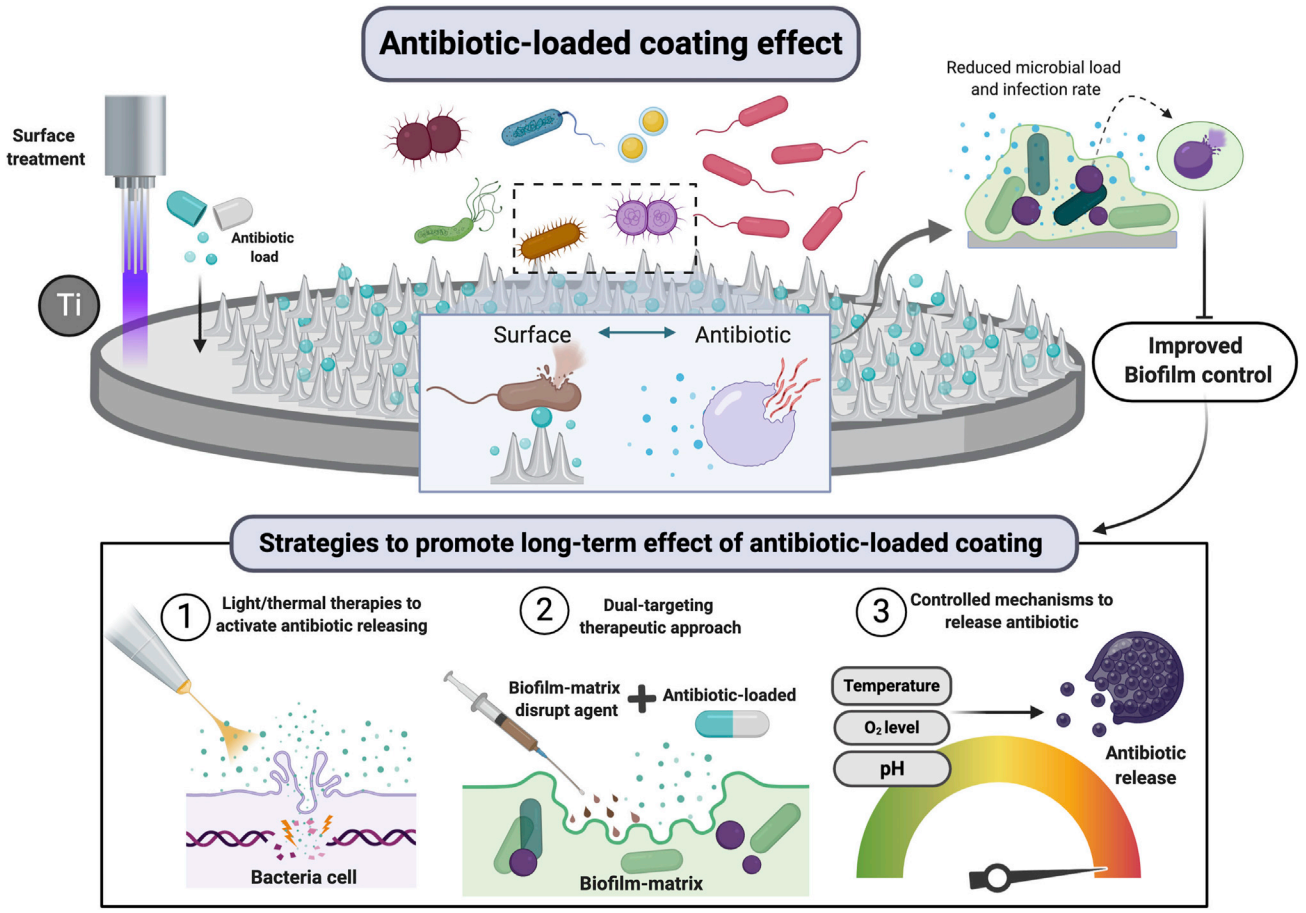

Figure 9. Schematic representation of the anti-biofilm activity of antibiotic-loaded coatings on titanium surface

Antibiotic loaded on titanium material by surface treatment may have bacteriostatic or bactericidal effect upon microbial contact with the antibiotic incorporated on the surface or by contact with the drug slowly released in the environment. This end result is reduction in microbial load of polymicrobial biofilms and, consequently, infection rates. Although a short-term releasing has been related to antibiotic-loaded coatings on titanium, some strategies (bottom panel) may promote drug releasing and antimicrobial effect, such as light therapies to activate the coating, dual-targeting therapies, and controlled mechanisms to release antibiotic (created by BioRender®).

Another possible way to overcome the limited long-term antimicrobial potential is the use of light-induced photocatalytic coatings, because it can be activated whenever infections are present (Nagay et al., 2019). Our previous study (Nagay et al., 2019) showed that titanium dioxide (TiO_2) surfaces doped with nitrogen (N) and bismuth (Bi) exhibited photocatalytic and antimicrobial activity only under visible light activation. Thus, when light activated, the electrons go into the TiO_2 molecule and move from the valence band to the conduction band, creating holes. It generates reactive oxygen species that are responsible to promote bacterial cell damage. This proposed surface also exhibited reusability of the photocatalyst, indicating that the surface can be reactivated several times. Jiang et al. (2020) recently developed a similar antibacterial photodynamic therapy where the antibiotics produce reactive oxygen species when under light irradiation. Taking the photocatalytic principle into consideration and the photosensitizer-like antibiotics, the combination of photocatalytic coatings loaded with these antibiotics might be a suitable strategy to reduce microbial accumulation onto implant surfaces under demand and can be activated whenever needed.

Therefore, as future challenges, the antibiotic-loaded coatings on Ti material should consider a long-term and sustained effect, the ability to reload the surface and to keep an effective local bacteriostatic and bactericidal effect at the implant surface without affecting the host-response or causing cytotoxicity to the host tissues surrounding the implants. Moreover, the most used antibiotics on coatings described in our systematic review, gentamicin and vancomycin, are not commonly used for oral infections due to their spectrum of action focusing on aerobic gram-negative bacilli. Thus, for dental implant applications, better

targeted antibiotics, such as amoxicillin and metronidazole, should be considered acting against gram negative, anaerobic bacteria that are relevant to peri-implantitis (Costa et al., 2020b).

Therefore, antibiotic-loaded coatings on Ti material are a promising approach to control implant-related infections, but some challenges, such as prolong effectiveness, enhanced surface properties, and effect on microbial load and in the microbial composition, need to be considered by future studies. In a nutshell, this review sheds light on potential alternative strategies aiming to reduce microbial loads and control polymicrobial infection on implanted devices.

Limitations of the study

The systematic review focused only on antibiotic-loaded coatings on titanium surface, but other antimicrobials agents can be used to achieve bacterial killing and prevent microbial infections. Moreover, dental implants can be made with different biomaterials, which was not considered in our systematic review. Finally, the studies included in our systematic review have some limitations. The antibiotic-loaded coatings evaluated require long-term evaluations by *in vitro*, animal and clinical models to determine their effect on reducing microbial loads and biofilm accumulation. Qualitative analysis of bacterial presence is not enough to assess anti-biofilm activity. Moreover, the effect of newly developed coatings on microbial composition needs to be evaluated, because dysbiotic biofilms are responsible for exacerbated inflammatory responses. In this attempt, microbiological assessment should consider the microbial diversity and environment that mimic the *in vivo* condition.

METHODS

All methods can be found in the accompanying Transparent Methods supplemental file.

SUPPLEMENTAL INFORMATION

Supplemental information can be found online at https://doi.org/10.1016/j.isci.2020.102008.

ACKNOWLEDGMENTS

This study was supported by the São Paulo Research Foundation (FAPESP) grant number 2020/05231-4 and the Brazilian National Council for Scientific and Technological Development (CNPq) grant number 304853/2018-6 to V.A.R.B., and NIH/NIDCR RO1DE013986 and NIH/NIGMS RO1GM127909 to A.D.B. Graphical abstract was created by BioRender®.

AUTHOR CONTRIBUTIONS

Conceptualization, J.G.S.S., M.B., A.D.B., and V.A.R.B.; Methodology, J.G.S.S., R.C.C., and B.E.N.; Investigation, J.G.S.S., M.B., R.C.C., and B.E.N.; Writing—Original Draft, J.G.S.S. and M.B.; Writing—Review & Editing, M.B., R.C.C., B.E.N., A.D.B., and V.A.R.B.; Supervision, A.D.B. and V.A.R.B.; Funding Acquisition, A.D.B. and V.A.R.B.

REFERENCES

Abusleme, L., Dupuy, A.K., Dutzan, N., Silva, N., Burleson, J.A., Strausbaugh, L.D., Gamonal, J., and Diaz, P.I. (2013). The subgingival microbiome in health and periodontitis and its relationship with community biomass and inflammation. ISME J. *7*, 1016–1025.

Albrektsson, T., and Wennerberg, A. (2004). Oral implant surfaces: Part 1–review focusing on topographic and chemical properties of different surfaces and in vivo responses to them. Int. J. Prosthodont. *17*, 536–543.

Adams, C.S., Antoci, V., Jr., Harrison, G., Patal, P., Freeman, T.A., Shapiro, I.M., Parvizi, J., Hickok, N.J., Radin, S., and Ducheyne, P. (2009). Controlled release of vancomycin from thin sol-gel films on implant surfaces successfully controls osteomyelitis. J. Orthop. Res. *27*, 701–709.

Alt, V., Kirchhof, K., Seim, F., Hrubesch, I., Lips, K.S., Mannel, H., Domann, E., and Schnettler, R. (2014). Rifampicin-fosfomycin coating for cementless endoprostheses: antimicrobial effects against methicillin-sensitive Staphylococcus aureus (MSSA) and methicillin-resistant Staphylococcus aureus (MRSA). Acta Biomater. *10*, 4518–4524.

Antoci, V., Jr., Adams, C.S., Hickok, N.J., Shapiro, I.M., and Parvizi, J. (2007). Vancomycin bound to Ti rods reduces periprosthetic infection: preliminary study. Clin. Orthop. Relat. Res. *461*, 88–95.

Arciola, C.R., Campoccia, D., and Montanaro, L. (2018). Implant infections: adhesion, biofilm formation and immune evasion. Nat. Rev. Microbiol. *16*, 397–409.

Auñón, Á., Esteban, J., Doadrio, A.L., Boiza-Sánchez, M., Mediero, A., Eguibar-Blázquez, D., Cordero-Ampuero, J., Conde, A., Arenas, M.Á., de-Damborenea, J.J., et al. (2020). Staphylococcus aureus prosthetic joint infection is prevented by a fluorine- and phosphorus-doped nanostructured Ti-6Al-4V alloy loaded with gentamicin and vancomycin. J. Orthop. Res. *38*, 588–597.

Aykut, S., Oztürk, A., Ozkan, Y., Yanik, K., Ilman, A.A., and Ozdemir, R.M. (2010). Evaluation and comparison of the antimicrobial efficacy of teicoplanin- and clindamycin-coated titanium implants: an experimental study. J. Bone Joint Surg. Br. *92*, 159–163.

Badar, M., Rahim, M.I., Kieke, M., Ebel, T., Rohde, M., Hauser, H., Behrens, P., and Mueller, P.P. (2015). Controlled drug release from antibiotic-loaded layered double

hydroxide coatings on porous titanium implants in a mouse model. J. Biomed. Mater. Res. A *103*, 2141–2149.

Berglundh, T., Armitage, G., Araujo, M.G., Avila-Ortiz, G., Blanco, J., Camargo, P.M., Chen, S., Cochran, D., Derks, J., Figuero, E., et al. (2018). Peri-implant diseases and conditions: consensus report of workgroup 4 of the 2017 world workshop on the classification of periodontal and peri-implant diseases and conditions. J. Clin. Periodontol. *45*, S286–S291.

Bertolini, M., Ranjan, A., Thompson, A., Diaz, P.I., Sobue, T., Maas, K., and Dongari-Bagtzoglou, A. (2019). Candida albicans induces mucosal bacterial dysbiosis that promotes invasive infection. PLoS Pathog. *15*, e1007717.

Bowen, W.H., Burne, R.A., Wu, H., and Koo, H. (2018). Oral biofilms: pathogens, matrix, and polymicrobial interactions in microenvironments. Trends Microbiol. *26*, 229–242.

Bürgers, R., Morsczeck, C., Felthaus, O., Gosau, M., Beck, H.C., and Reichert, T.E. (2018). Induced surface proteins of Staphylococcus epidermidis adhering to titanium implant substrata. Clin. Oral Investig. *22*, 2663–2668.

Canullo, L., Radovanović, S., Delibasic, B., Blaya, J.A., Penarrocha, D., and Rakic, M. (2017). The predictive value of microbiological findings on teeth, internal and external implant portions in clinical decision making. Clin. Oral Implants Res. *28*, 512–519.

Cao, Y., Su, B., Chinnaraj, S., Jana, S., Bowen, L., Charlton, S., Duan, P., Jakubovics, N.S., and Chen, J. (2018). Nanostructured titanium surfaces exhibit recalcitrance towards Staphylococcus epidermidis biofilm formation. Sci. Rep. *8*, 1071.

Carcuac, O., Derks, J., Charalampakis, G., Abrahamsson, I., Wennström, J., and Berglundh, T. (2016). Adjunctive systemic and local antimicrobial therapy in the surgical treatment of peri-implantitis: a randomized controlled clinical trial. J. Dent. Res. *95*, 50–57.

Ccahuana-Vásquez, R.A., Tabchoury, C.P., Tenuta, L.M., Del Bel Cury, A.A., Vale, G.C., and Cury, J.A. (2007). Effect of frequency of sucrose exposure on dental biofilm composition and enamel demineralization in the presence of fluoride. Caries Res. *41*, 9–15.

Chang, Y.Y., Zhang, J.H., and Huang, H.L. (2018). Effects of laser texture oxidation and high-temperature annealing of TiV alloy thin films on mechanical and antibacterial properties and cytotoxicity. Materials (Basel) *11*, 2495.

Cheng, Y., Feng, G., and Moraru, C.I. (2019). Micro- and nanotopography sensitive bacterial attachment mechanisms: a review. Front. Microbiol. *10*, 191.

Chouirfa, H., Bouloussa, H., Migonney, V., and Falentin-Daudré, C. (2019). Review of titanium surface modification techniques and coatings for antibacterial applications. Acta Biomater. *83*, 37–54.

Costa, R.C., Souza, J.G.S., Cordeiro, J.M., Bertolini, M., de Avila, E.D., Landers, R., Rangel, E.C., Fortulan, C.A., Retamal-Valdes, B., da Cruz, N.C., et al. (2020a). Synthesis of bioactive glass-based coating by plasma electrolytic oxidation: untangling a new deposition pathway toward titanium implant surfaces. J. Colloid Interface Sci. *579*, 680–698.

Costa, R.C., Souza, J.G.S., Bertolini, M., Retamal-Valdes, B., Feres, M., and Barão, V.A.R. (2020b). Extracellular biofilm matrix leads to microbial dysbiosis and reduces biofilm susceptibility to antimicrobials on titanium biomaterial: an in vitro and in situ study. Clin. Oral Implants Res. *31*, 1173–1186.

Costerton, J.W., Lewandowski, Z., Caldwell, D.E., Korber, D.R., and Lappin-Scott, H.M. (1995). Microbial biofilms. Annu. Rev. Microbiol. *49*, 711–745.

Croes, M., Bakhshandeh, S., van Hengel, I., Lietaert, K., van Kessel, K., Pouran, B., van der Wal, B., Vogely, H.C., Van Hecke, W., Fluit, A.C., et al. (2018). Antibacterial and immunogenic behavior of silver coatings on additively manufactured porous titanium. Acta Biomater. *81*, 315–327.

Dabdoub, S.M., Tsigarida, A.A., and Kumar, P.S. (2013). Patient-specific analysis of periodontal and peri-implant microbiomes. J. Dent. Res. *92*, 168S-75S.

Darouiche, R.O., Mansouri, M.D., Zakarevicz, D., Alsharif, A., and Landon, G.C. (2007). In vivo efficacy of antimicrobial-coated devices. J. Bone Joint Surg. Am. *89*, 792–797.

Darouiche, R.O. (2004). Treatment of infections associated with surgical implants. N. Engl. J. Med. *350*, 1422–1429.

Davidson, H., Poon, M., Saunders, R., Shapiro, I.M., Hickok, N.J., and Adams, C.S. (2015). Tetracycline tethered to titanium inhibits colonization by gram-negative bacteria. J. Biomed. Mater. Res. B Appl. Biomater. *103*, 1381–1389.

Dewhirst, F.E., Chen, T., Izard, J., Paster, B.J., Tanner, A.C., Yu, W.H., Lakshmanan, A., and Wade, W.G. (2010). The human oral microbiome. J. Bacteriol. *192*, 5002–5017.

Diefenbeck, M., Schrader, C., Gras, F., Mückley, T., Schmidt, J., Zankovych, S., Bossert, J., Jandt, K.D., Völpel, A., Sigusch, B.W., et al. (2016). Gentamicin coating of plasma chemical oxidized titanium alloy prevents implant-related osteomyelitis in rats. Biomaterials *101*, 156–164.

Dodo, C.G., Senna, P.M., Custodio, W., Paes Leme, A.F., and Del Bel Cury, A.A. (2013). Proteome analysis of the plasma protein layer adsorbed to a rough titanium surface. Biofouling *29*, 549–557.

Fenton, O.S., Olafson, K.N., Pillai, P.S., Mitchell, M.J., and Langer, R. (2018). Advances in biomaterials for drug delivery. Adv. Mater. e1705328.

Feres, M., Figueiredo, L.C., Soares, G.M., and Faveri, M. (2015). Systemic antibiotics in the treatment of periodontitis. Periodontol *2000* (67), 131–186.

Ferraris, S., and Spriano, S. (2016). Antibacterial titanium surfaces for medical implants. Mater. Sci. Eng. C Mater. Biol. Appl. *61*, 965–978.

Figuero, E., Graziani, F., Sanz, I., Herrera, D., and Sanz, M. (2014). Management of peri-implant mucositis and peri-implantitis. Periodontol *2000* (66), 255–273.

Flemming, H.C., and Wingender, J. (2010). The biofilm matrix. Nat. Rev. Microbiol. *8*, 623–633.

Franz, S., Rammelt, S., Scharnweber, D., and Simon, J.C. (2011). Immune responses to implants - a review of the implications for the design of immunomodulatory biomaterials. Biomaterials *32*, 6692–6709.

Fürst, M.M., Salvi, G.E., Lang, N.P., and Persson, G.R. (2007). Bacterial colonization immediately after installation on oral titanium implants. Clin. Oral Implants Res. *18*, 501–508.

Ghimire, A., Skelly, J.D., and Song, J. (2019). Micrococcal-nuclease-triggered on-demand release of vancomycin from intramedullary implant coating eradicates Staphylococcus aureus infection in mouse femoral canals. ACS Cent. Sci. *5*, 1929–1936.

Grohmann, S., Menne, M., Hesse, D., Bischoff, S., Schiffner, R., Diefenbeck, M., and Liefeith, K. (2019). Biomimetic multilayer coatings deliver gentamicin and reduce implant-related osteomyelitis in rats. Biomed. Tech. (Berl) *64*, 383–395.

Heitz-Mayfield, L.J., and Mombelli, A. (2014). The therapy of peri-implantitis: a systematic review. Int. J. Oral Maxillofac. Implants *29*, 325–345.

Heitz-Mayfield, L.J., and Lang, N.P. (2010). Comparative biology of chronic and aggressive periodontitis vs. peri-implantitis. Periodontol *2000* (53), 167–181.

Hickok, N.J., and Shapiro, I.M. (2012). Immobilized antibiotics to prevent orthopaedic implant infections. Adv. Drug Deliv. Rev. *64*, 1165–1176.

Janson, O., Sörensen, J.H., Strømme, M., Engqvist, H., Procter, P., and Welch, K. (2019). Evaluation of an alkali-treated and hydroxyapatite-coated orthopedic implant loaded with tobramycin. J. Biomater. Appl. *34*, 699–720.

Jenkinson, H.F. (2011). Beyond the oral microbiome. Environ. Microbiol. *13*, 3077–3087.

Jennings, J.A., Beenken, K.E., Skinner, R.A., Meeker, D.G., Smeltzer, M.S., Haggard, W.O., and Troxel, K.S. (2016). Antibiotic-loaded phosphatidylcholine inhibits staphylococcal bone infection. World J. Orthop. *18*, 467–474.

Jiang, Q.I., Fangiie, E., Tian, J., Yang, J., Zhang, J., and Che, Y. (2020). Light-excited antibiotics for potentiating bacterial killing via reactive oxygen species generation. ACS Appl. Mater. Interfaces *12*, 16150–16158.

Kalasin, S., and Santore, M.M. (2009). Non-specific adhesion on biomaterial surfaces driven by small amounts of protein adsorption. Colloids Surf. B Biointerfaces *73*, 229–236.

Kälicke, T., Schierholz, J., Schlegel, U., Frangen, T.M., Köller, M., Printzen, G., Seybold, D., Klöckner, S., Muhr, G., and Arens, S. (2006). Effect

on infection resistance of a local antiseptic and antibiotic coating on osteosynthesis implants: an in vitro and in vivo study. J. Orthop. Res. *24*, 1622–1640.

Khan, S.T., Al-Khedhairy, A.A., and Musarrat, J. (2015). ZnO and TiO2 nanoparticles as novel antimicrobial agents for oral hygiene: a review. J. Nanopart. Res. *17*, 276.

Kolenbrander, P.E., Palmer, R.J., Rickard, A.H., Jakubovics, N.S., Chalmers, N.I., and Diaz, P. (2006). Bacterial interactions and successions during plaque development. Periodontol *2000* (42), 47–79.

Koo, H., Falsetta, M.L., and Klein, M.I. (2013). The exopolysaccharide matrix: a virulence determinant of cariogenic biofilm. J. Dent. Res. *92*, 1065–1073.

Koo, H., Allan, R.N., Howlin, R.P., Stoodley, P., and Hall-Stoodley, L. (2017). Targeting microbial biofilms: current and prospective therapeutic strategies. Nat. Rev. Microbiol. *15*, 740–755.

Kucharíková, S., Gerits, E., De Brucker, K., Braem, A., Ceh, K., Majdic, G., Spanic, T., Pogorovec, E., Verstraeten, N., Tournu, H., et al. (2016). Covalent immobilization of antimicrobial agents on titanium prevents Staphylococcus aureus and Candida albicans colonization and biofilm formation. J. Antimicrob. Chemother. *71*, 936–945.

Kumar, P.S., Mason, M.R., Brooker, M.R., and O'Brien, K. (2012). Pyrosequencing reveals unique microbial signatures associated with healthy and failing dental implants. J. Clin. Periodontol. *39*, 425–433.

Lang, N.P., Bragger, U., Walther, D., Beamer, B., and Kornman, K.S. (1993). Ligature-induced peri-implant infection in cynomolgus monkeys. I. Clinical and radiographic findings. Clin. Oral Implants Res. *4*, 2–11.

Lendenmann, U., Grogan, J., and Oppenheim, F.G. (2000). Saliva and dental pellicle—a review. Adv. Dent. Res. *14*, 22–28.

Leonhardt, A., Renvert, S., and Dahlen, G. (1999). Microbial findings at failing implants. Clin. Oral Implants Res. *10*, 339–345.

Li, D., Ferguson, S.J., Beutler, T., Cochran, D.L., Sittig, C., Hirt, H.P., and Buser, D. (2002). Biomechanical comparison of the sandblasted and acid-etched and the machined and acid-etched titanium surface for dental implants. J. Biomed. Mater. Res. *60*, 325–332.

Lima, E.M., Koo, H., Vacca Smith, A.M., Rosalen, P.L., and Del Bel Cury, A.A. (2008). Adsorption of salivary and serum proteins, and bacterial adherence on titanium and zirconia ceramic surfaces. Clin. Oral Implants Res. *19*, 780–785.

Lindhe, J., Berglundh, T., Ericsson, I., Liljenberg, B., and Marinello, C. (1992). Experimental breakdown of peri-implant and periodontal tissues. A study in the beagle dog. Clin. Oral Implants Res. *3*, 9–16.

Liu, D., He, C., Liu, Z., and Xu, W. (2017). Gentamicin coating of nanotubular anodized titanium implant reduces implant-related osteomyelitis and enhances bone biocompatibility in rabbits. Int. J. Nanomedicine *12*, 5461–5471.

Lorenzetti, M., Dogša, I., Stošicki, T., Stopar, D., Kalin, M., Kobe, S., and Novak, S. (2015). The influence of surface modification on bacterial adhesion to titanium-based substrates. ACS Appl. Mater. Interfaces *7*, 1644–1651.

Lucke, M., Schmidmaier, G., Sadoni, S., Wildemann, B., Schiller, R., Haas, N.P., and Raschke, M. (2003). Gentamicin coating of metallic implants reduces implant-related osteomyelitis in rats. Bone *32*, 521–531.

Lucke, M., Wildemann, B., Sadoni, S., Surke, C., Schiller, R., Stemberg, A., Raschke, M., Haas, N.P., and Schmidmaier, G. (2005). Systemic versus local application of gentamicin in prophylaxis of implant-related osteomyelitis in a rat model. Bone *36*, 770–778.

Ma, K., Cai, X., Zhou, Y., Wang, Y., and Jiang, T. (2017). In vitro and in vivo evaluation of tetracycline loaded chitosan-gelatin nanosphere coatings for titanium surface functionalization. Macromol. Biosci. *17*, 2.

Marsh, P.D., and Devine, D.A. (2011). How is the development of dental biofilms influenced by the host? J. Clin. Periodontol. *38*, 28–35.

Marsh, P.D., Moter, A., and Devine, D.A. (2011). Dental plaque biofilms: communities, conflict and control. Periodontol *2000* (55), 16–35.

Matos, A.O., Ricomini-Filho, A.P., Beline, T., Ogawa, E.S., Costa-Oliveira, B.E., Almeida, A.B., Nociti Junior, F.H., Rangel, E.C., da Cruz, N.C., Sukotjo, C., et al. (2017). Three-species biofilm model onto plasma-treated titanium implant surface. Colloids Surf. B Biointerfaces *152*, 354–366.

Melo, F., Nascimento, C., Souza, D.O., and Albuquerque, R.F. (2017). Identification of oral bacteria on titanium implant surfaces by 16S rDNA sequencing. Clin. Oral Implants Res. *28*, 697–703.

Mercado, F., Hamlet, S., and Ivanovski, S. (2018). Regenerative surgical therapy for peri-implantitis using deproteinized bovine bone mineral with 10% collagen, enamel matrix derivative and doxycycline-A prospective 3-year cohort study. Clin. Oral Implants Res. *29*, 583–591.

Metsemakers, W.J., Emanuel, N., Cohen, O., Reichart, M., Potapova, I., Schmid, T., Segal, D., Riool, M., Kwakman, P.H.S., Boer, L., et al. (2015). A doxycycline-loaded polymer-lipid encapsulation matrix coating for the prevention of implant-related osteomyelitis due to doxycycline-resistant methicillin-resistant Staphylococcus aureus. J. Control Release *209*, 47–56.

Mombelli, A., and Décaillet, F. (2011). The characteristics of biofilms in peri-implant disease. J. Clin. Periodontol. *38*, 203–213.

Moskowitz, J.S., Blaisse, M.R., Samuel, R.E., Hsu, H.P., Harris, M.B., Martin, S.D., Lee, J.C., Spector, M., and Hammond, P.T. (2010). The effectiveness of the controlled release of gentamicin from polyelectrolyte multilayers in the treatment of Staphylococcus aureus infection in a rabbit bone model. Biomaterials *31*, 6019–6030.

Nagay, B.E., Dini, C., Cordeiro, J.M., Ricomini-Filho, A.P., Avila, E.D., Rangel, E.C., Cruz, N.C., and Barao, V.A.R. (2019). Visible-light-induced photocatalytic and antibacterial activity of TiO 2 codoped with nitrogen and bismuth: new perspectives to control implant-biofilm-related diseases. ACS Appl. Mater. Inter. *11*, 18186–18202.

Naginyte, M., Do, T., Meade, J., Devine, D.A., and Marsh, P.D. (2019). Enrichment of periodontal pathogens from the biofilms of healthy adults. Sci. Rep. *9*, 1–9.

Neut, D., Dijkstra, R.J., Thompson, J.I., Kavanagh, C., van der Mei, H.C., and Busscher, H.J. (2015). A biodegradable gentamicin-hydroxyapatite-coating for infection prophylaxis in cementless hip prostheses. Eur. Cell. Mater *29*, 42–56.

Nguyen, Vo., Hao, J., Chou, J., Oshima, M., Aoki, K., Kuroda, S., Kaboosaya, B., and Kasugai, S. (2017). Ligature induced peri-implantitis: tissue destruction and inflammatory progression in a murine model. Clin. Oral Implants Res. *28*, 129–136.

Nie, B., Ao, H., Long, T., Zhou, J., Tang, T., and Yue, B. (2017). Immobilizing bacitracin on titanium for prophylaxis of infections and for improving osteoinductivity: an in vivo study. Colloids Surf. B Biointerfaces *150*, 183–191.

Nie, B., Long, T., Ao, H., Zhou, J., Tang, T., and Yue, B. (2016). Covalent immobilization of enoxacin onto titanium implant surfaces for inhibiting multiple bacterial species infection and in vivo methicillin-resistant Staphylococcus aureus infection prophylaxis. Antimicrob. Agents Chemother. *61*, e01766–16.

Oliva, A., Pavone, P., D'Abramo, A., Iannetta, M., Mastroianni, C.M., and Vullo, V. (2016). Role of sonication in the microbiological diagnosis of implant-associated infections: beyond the orthopedic prosthesis. Adv. Exp. Med. Biol. *897*, 85–102.

Oliveira, W.F., Silva, P.M.S., Silva, R.C.S., Silva, G.M.M., Machado, G., Coelho, L.C.B.B., and Correia, M.T.S. (2018). Staphylococcus aureus and Staphylococcus epidermidis infections on implants. J. Hosp. Infect. *98*, 111–117.

Padial-Molina, M., Lopez-Martinez, J., OValle, F., and Galindo-Moreno, P. (2016). Microbial profiles and detection techniques in peri-implant diseases: a systematic review. J. Oral Maxillofac. Res. *7*, e10.

Pantaroto, H.N., Amorim, K.P., Cordeiro, J.M., Souza, J.G.S., Ricomini-Filho, A.P., Rangel, E.C., and Barao, V.A.R. (2019). Proteome analysis of the salivary pellicle formed on titanium alloys containing niobium and zirconium. Biofouling *35*, 173–186.

Perni, S., Alotaibi, H.F., Yergeshov, A.A., Dang, T., Abdullin, T.I., and Prokopovich, P. (2020). Long acting anti-infection constructs on titanium. J. Control Release. *326*, 91–105.

Pokrowiecki, R. (2018). The paradigm shift for drug delivery systems for oral and maxillofacial implants. Drug Deliv. *25*, 1504–1515.

Puckett, S.D., Taylor, E., Raimondo, T., and Webster, T.J. (2010). The relationship between the nanostructure of titanium surfaces and bacterial attachment. Biomaterials *31*, 706–713.

Rabe, M., Verdes, D., and Seeger, S. (2011). Understanding protein adsorption phenomena at solid surfaces. Adv. Colloid Interface Sci. *162*, 87–106.

Renvert, S., Lessem, J., Dahlen, G., Lindahl, C., and Svensson, M. (2006). Topical minocycline microspheres versus topical chlorhexidine gel as an adjunct to mechanical debridement of incipient peri-implant infections: a randomized clinical trial. J. Clin. Periodontol. *33*, 362–369.

Retamal-Valdes, B., Formiga, M.C., Almeida, M.L., Fritoli, A., Figueiredo, K.A., Westphal, M., Gomes, P., and Feres, M. (2019). Does subgingival bacterial colonization differ between implants and teeth? A systematic review. Braz. Oral Res. *33*, e064.

Romero-Gavilán, F., Gomes, N.C., Ródenas, J., Sánchez, A., Azkargorta, M., Iloro, I., Elortza, F., Arnáez, I.A., Gurruchaga, M., Goñi, I., and Suay, I. (2017). Proteome analysis of human serum proteins adsorbed onto different titanium surfaces used in dental implants. Biofouling *33*, 98–111.

Rosier, B.T., Marsh, P.D., and Mira, A. (2018). Resilience of the oral microbiota in health: mechanisms that prevent dysbiosis. J. Dent. Res. *97*, 371–380.

Salvi, G.E., Cosgarea, R., and Sculean, A. (2017). Prevalence and mechanisms of peri-implant diseases. J. Dent. Res. *96*, 31–37.

Schincaglia, G.P., Hong, B.Y., Rosania, A., Barasz, J., Thompson, A., Panagakos, F., Burleson, J.A., Dongari-Bagtzoglou, A., and Diaz, P.I. (2017). Clinical, immune, and microbiome traits of gingivitis and peri-implant mucositis. J. Dent. Res. *96*, 47–55.

Schmidlin, P.R., Muller, P., Attin, T., Wieland, M., Hofer, D., and Guggenheim, B. (2013). Polyspecies biofilm formation on implant surfaces with different surface characteristics. J. Appl. Oral Sci. *21*, 48–55.

Schou, S., Holmstrup, P., Hjørting-Hansen, E., and Kornman, K.S. (1993). Ligature-induced marginal inflammation around osseointegrated implants and ankylosed teeth. Clin. Oral Implant Res. *4*, 12–22.

Schwarz, F., Becker, K., Rahn, S., Hegewald, A., Pfeffer, K., and Henrich, B. (2015). Real-time PCR analysis of fungal organisms and bacterial species at peri-implantitis sites. Int. J. Implant Dent *1*, 9.

Shibli, J.A., Melo, L., Ferrari, D.S., Figueiredo, L.C., Faveri, M., and Feres, M. (2008). Composition of supra-and subgingival biofilm of subjects with healthy and diseased Implants. Clin. Oral Implants Res. *19*, 975–982.

Shibli, J.A., Ferrari, D.S., Siroma, R.S., Figueiredo, L.C., Faveri, M., and Feres, M. (2019). Microbiological and clinical effects of adjunctive systemic metronidazole and amoxicillin in the non-surgical treatment of peri-implantitis: 1 year follow-up. Braz. Oral Res. *33*, 080.

Smith, F.R.C., Riollano, M., Leung, A., and Hammond, P.T. (2009). Layer-by-layer platform technology for small-molecule delivery. Angew. Chem. Int. Ed. Eng. *48*, 8974–8977.

Socransky, S.S., and Haffajee, A.D. (2002). Dental biofilms: difficult therapeutic targets. Periodontol *2000* (28), 12–55.

Song, F., Koo, H., and Ren, D. (2015). Effects of material properties on bacterial adhesion and biofilm formation. J. Dent. Res. *94*, 1027–1034.

Song, W., Seta, J., Chen, L., Bergum, C., Zhou, Z., Kanneganti, P., Kast, R.E., Auner, G.W., Shen, M., Markel, D.C., et al. (2017). Doxycycline-loaded coaxial nanofiber coating of titanium implants enhances osseointegration and inhibits Staphylococcus aureus infection. Biomed. Mater. *12*, 045008.

Souza, J.G.S., Bertolini, M., Costa, R.C., Lima, C.V., and Barão, V.A.R. (2020a). Proteomic profile of the saliva and plasma protein layer adsorbed on Ti-Zr alloy: the effect of sandblasted and acid-etched surface treatment. Biofouling *36* (4), 428–444.

Souza, J.G.S., Bertolini, M., Costa, R.C., Cordeiro, J.M., Nagay, B.E., Almeida, A.B., Retamal-Valdes, B., Nociti, F.H., Feres, M., Rangel, E.C., and Barão, V.A.R. (2020b). Targeting pathogenic biofilms: newly developed superhydrophobic coating favors a host-compatible microbial profile on the titanium surface. ACS Appl. Mater. Interfaces *12*, 10118–10129.

Souza, J.G.S., Bertolini, M., Thompson, A., Barão, V.A.R., and Dongari-Bagtzoglou, A. (2020c). Biofilm interactions of Candida albicans and mitis group streptococci in a titanium-mucosal interface model. Appl. Environ. Microbiol. *86*, e02950–19.

Souza, J.G.S., Bertolini, M., Thompson, A., Mansfield, J.M., Grassmann, A.A., Maas, K., Caimano, M.J., Barão, V.A.R., Vickerman, M.M., and Dongari-Bagtzoglou, A. (2020d). Role of glucosyltransferase R in biofilm interactions between Streptococcus oralis and Candida albicans. ISME J. *14*, 1207–1222.

Souza, J.G.S., Costa-Oliveira, B.E., Bertolini, M., Lima, C.V., Retamal-Valdes, B., Faveri, M., Feres, M., and Barão, V.A. (2020e). Titanium particles and ions favor dysbiosis in oral biofilms. J. Periodontal Res. *55*, 258–266.

Souza, J.G.S., Cury, J.A., Ricomini Filho, A.P., Feres, M., Faveri, M., and Barão, V.A.R. (2019a). Effect of sucrose on biofilm formed in situ on titanium material. J. Periodontol. *90*, 141–148.

Souza, J.G.S., Cordeiro, J.M., Lima, C.V., and Barão, V.A.R. (2019b). Citric acid reduces oral biofilm and influences the electrochemical behavior of titanium: an in situ and in vitro study. J. Periodontol. *90*, 149–158.

Souza, J.G.S., Lima, C.V., Costa-Oliveira, B.E., Ricomini-Filho, A.P., Faveri, M., Sukotjo, C., Feres, M., Del Bel Cury, A.A., and Barão, V.A.R. (2018). Dose-response effect of chlorhexidine on a multispecies oral biofilm formed on pure titanium and on a titanium-zirconium alloy. Biofouling *34*, 1175–1184.

Spriano, S., Yamaguchi, S., Baino, F., and Ferraris, S. (2018). A critical review of multifunctional titanium surfaces: new frontiers for improving osseointegration and host response, avoiding bacteria contamination. Acta Biomater. *79*, 1–22.

Stavrakis, A.I., Zhu, S., Loftin, A.H., Weixian, X., Niska, J., Hegde, V., Segura, T., and Bernthal, N.M. (2019). Controlled release of vancomycin and tigecycline from an orthopaedic implant coating prevents Staphylococcus aureus infection in an open fracture animal model. Biomed. Res. Int. *2019*, 1638508.

Stevanović, M., Djošić, M., Janković, A., Kojić, V., Vukašinović-Sekulić, M., Stojanović, J., Odović, J., Sakač, M.C., Rhee, K.Y., and Mišković-Stanković, V. (2020). Antibacterial graphene-based hydroxyapatite/chitosan coating with gentamicin for potential applications in bone tissue engineering. J. Biomed. Mater. Res. A. *108*, 2175–2189.

Sultan, A.S., Kong, E.F., Rizk, A.M., and Jabra-Rizk, M.A. (2018). The oral microbiome: a Lesson in coexistence. PLoS Pathog. *14*, e1006719.

Thompson, K., Petkov, S., Zeiter, S., Sprecher, C.M., Richards, R.G., Moriarty, T.F., and Eijer, H. (2019). Intraoperative loading of calcium phosphate-coated implants with gentamicin prevents experimental Staphylococcus aureus infection in vivo. PLoS One *14*, e0210402.

Van Winkelhoff, A.J. (2012). Antibiotics in the treatment of peri-implantitis. Eur. J. Oral Implantol. *5*, S43–S50.

Welch, J.L.M., Dewhirst, F.E., and Borusy, G.G. (2019). Biogeography of the oral microbiome: the site-specialist hypothesis. Annu. Rev. Microbiol. *73*, 335–358.

Whitehead, K.A., Rogers, D., Colligon, J., Wright, C., and Verran, J. (2006). Use of the atomic force microscope to determine the effect of substratum surface topography on the ease of bacterial removal. Colloids Surf. B Biointerfaces *51*, 44–53.

Whittaker, C.J., Klier, C.M., and Kolenbrander, P.E. (1996). Mechanisms of adhesion by oral bacteria. Annu. Rev. Microbiol. *50*, 513–552.

Williams, R.C., Paquette, D.W., Offenbacher, S., Adams, D.F., Armitage, G.C., Bray, K., Caton, J., Cochran, D.L., Drisko, C.H., Fiorellini, J.P., et al. (2001). Treatment of periodontitis by local administration of minocycline microspheres: a controlled trial. J. Periodontol. *72*, 1535–1544.

Xiao, J., Klein, M.I., Falsetta, M.L., Lu, B., Delahunty, C.M., Yates, J.R., Heydorn, A., and Koo, H. (2012). The exopolysaccharide matrix modulates the interaction between 3D architecture and virulence of a mixed-species oral biofilm. PLoS Pathog. *8*, e1002623.

Xu, H., Sobue, T., Thompson, A., Xie, Z., Poon, K., Ricker, A., Cervantes, J., Diaz, P.I., and Dongari-Bagtzoglou, A. (2014a). Streptococcal co-infection augments Candida pathogenicity by amplifying the mucosal inflammatory response. Cell. Microbiol. *16*, 214–231.

Xu, H., Jenkinson, H.F., and Dongari-Bagtzoglou, A. (2014b). Innocent until proven guilty: mechanisms and roles of Streptococcus-Candida

interactions in oral health and disease. Mol. Oral Microbiol. *29*, 99–116.

Yang, Y., Ao, H.Y., Yang, S.B., Wang, Y.G., Lin, W.T., Yu, Z.F., and Tang, T.T. (2016). In vivo evaluation of the anti-infection potential of gentamicin-loaded nanotubes on titania implants. Int. J. Nanomedicine *11*, 2223–2234.

Yu, T.S. (2004). Effect of titanium-ion on the growth of various bacterial species. J. Microbiol. *42*, 47–50.

Yuan, Z., Huang, S., Lan, S., Xiong, H., Tao, B., Ding, Y., Liu, Y., Liu, P., and Cai, K. (2018). Surface engineering of titanium implants with enzyme-triggered antibacterial properties and enhanced osseointegration in vivo. J. Mater. Chem. B *6*, 8090–8140.

Zaura, E., Keijser, B.J.F., Huse, S.M., and Crielaard, W. (2009). Defining the healthy "core microbiome" of oral microbial communities. BMC Microbiol. *9*, 259.

Zeng, J., Wang, Y., Sun, Z., Chang, H., Cao, M., Lin, K., and Xie, Y. (2020). A novel biocompatible PDA/IR820/DAP coating for antibiotic/photodynamic/photothermal triple therapy to inhibit and eliminate Staphylococcus aureus biofilm. Chem. Eng. *394*, 1250172.

Zhang, B., Braun, B.M., Skelly, J.D., Ayers, D.C., and Song, J. (2019). Significant suppression of Staphylococcus aureus colonization on intramedullary Ti6Al4V implants surface-grafted with vancomycin-bearing polymer brushes. ACS Appl. Mater. Interfaces *11*, 28641–28647.

Zhang, H., Wang, G., Liu, P., Tong, D., Ding, C., Zhang, Z., Xie, Y., Tang, H., and Ji, H. (2018). Vancomycin-loaded titanium coatings with an interconnected micro-patterned structure for prophylaxis of infections: an in vivo study. RSC Adv. *8*, 9223–9231.

Zhou, L., Liu, Q., Zhou, Z., Lu, W., and Tao, J. (2017). Efficacy of tobramycin-loaded coating K-wire in an open-fracture rabbit model contaminated by staphylococcus aureus. Int. J. Clin. Exp. Med. *10*, 6004–6016.

Zitzmann, N.U., Berglundh, T., Marinello, C.P., and Lindhe, J. (2001). Experimental peri-implant mucositis in man. J. Clin. Periodontol. *28*, 517–523.

iScience, Volume *24*

Supplemental Information

Targeting implant-associated infections:

titanium surface loaded with antimicrobial

João Gabriel Silva Souza, Martinna Mendonça Bertolini, Raphael Cavalcante Costa, Bruna Egumi Nagay, Anna Dongari-Bagtzoglou, and Valentim Adelino Ricardo Barão

Transparent Methods

Materials and methods

This systematic review was conducted in order to answer the following focused question: *"Do antibiotic-loaded coatings on titanium surface reduce long-term peri-implant infection?"*. This study was performed according to PRISMA statement recommendations for the report of systematic reviews.

Search strategy

An extensive literature search was performed among six electronic databases up to May 9, 2020: PubMed (MEDLINE), Scopus, Web of Science, The Cochrane Library, and Embase. The grey literature was also searched by the System for Information on Grey Literature in Europe (SIGLE) through the OpenGrey. The entire electronic strategy was developed with MeSH terms/entry terms and free terms appropriately combine by boolean operators (OR; AND) and adapted for each database (Please see Supplemental material – Table S1, related Figure 6). The present systematic review and the search strategy was developed with no language and publication time restriction. A manual screening of the reference list of all included studies was performed, preventing any missing articles. Expert authors were contacted for information of ongoing studies and not published data. Additionally, to keep the search strategy up-to-date, alerts were established for each database.

Eligibility criteria

For the systematic review, the studies had to meet the following inclusion criteria: (a) to evaluate antibiotic-loaded coatings on Ti based-material implants; (b) to have a control group with untreated implants or not loaded with antibiotic; (c) to report primary outcomes related to microbial assessment such as biofilm/microbial load (quantitative data) and implant contamination rate. Studies not meeting the inclusion criteria were excluded. Additionally, the studies designated as literature reviews, case reports, case series, in vitro, in silico, descriptive and observational were also excluded. The PICO strategy described below was used:

(P) – Population: humans or animals with Ti based-implants;

(I) – Intervention: surface treatment with antibiotic on Ti implants clearly described;

(C) – Comparison: control (not treated/loaded with antibiotic) implants; and,

(O) – Outcome: biofilm load (bacterial counts, area covered by biofilm, bioluminescence intensity, biovolume or plaque index) and implant contamination rate (bacterial presence).

Study selection

References recorded identified through all databases were imported to Mendeley reference manager (Mendeley Desktop, v1.19.4; Elsevier). Duplicate entries were excluded according to authors' names, the titles of references and year of publication. After elimination of duplicate entries, two reviewers (R. C. C. and B. E. N.) independently screened all titles and abstracts for possible inclusion. In cases of insufficient information provided in papers' abstracts, the full paper was read to evaluate its eligibility. Subsequently, full texts of the remaining papers were analyzed and those that met the inclusion criteria were included. The agreement between the two reviewers regarding the titles and abstracts selection as well as full text was evaluated by Cohen's kappa coefficient (κ). Any disagreements were resolved by discussion and a third author (J. G. S. S.) was consulted to reach a consensus about eligibility.

Data extraction process

Data from the included studies were independently recorded: study features (author(s) and year of publication), animal (species, n value and infection presence), implant information (Ti based-material, surgical site, surface treatment, antibiotic load), time of follow-up, peri-implant infection rate, drug concentration loaded in the surface, in vitro drug release, and microbiological tests characterized by mean and standard deviation. In case of missing data, the corresponding authors were contacted via institutional e-mail and ResearchGate® website. Some papers from the same study were associated under a single report (the most recent publication). For available data only in graphs with no mean and standard deviation exact values, data were extracted using the program WebPlotDigitizer which is considered a reliable tool for data extraction (Burda et al., 2016).

Supplemental Items:

TABLE S1. Search strategy according to different databases, related to the main text and Figure 6.

PubMed (n = 325)	Scopus (n = 522)	Web of Science (n = 413)	Cochrane Library (n = 29)	Embase (n = 229)	OPENGREY (n = 0)
#1 ((((Titanium[MeSH Terms]) OR (Titanium[Title/Abstract])) OR (Titania[Title/Abstract])) AND ((((((Coated materials, biocompatible[MeSH Terms]) OR (coat*[Title/Abstract])) OR (film*[Title/Abstract])) OR (deposit*[Title/Abstract])) OR (surface* treat*[Title/Abstract]) OR (treat* surface*)) **#2** ((((((((((((((((((Antibiotic*[Title/Abstract]) OR (Amoxicillin[Title/Abstract])) OR (Penicillin[Title/Abstract])) OR (Azithromycin[Title/Abstract])) OR (Clarithromycin[Title/Abstract])) OR (Anthracycline*[Title/Abstract])) OR (Gentamicin*[Title/Abstract])) OR (Neomycin[Title/Abstract])) OR (Streptomycin[Title/Abstract])) OR (Streptozocin[Title/Abstract])) OR (Tobramycin[Title/Abstract])) OR (Vancomycin[Title/Abstract])) OR (Ciprofloxacin[Title/Abstract])) OR (Enrofloxacin[Title/Abstract])) OR (Clindamycin[Title/Abstract])) OR (Metronidazole[Title/Abstract])) OR (Doxycycline[Title/Abstract])) OR (Minocycline[Title/Abstract])) OR (Tetracycline[Title/Abstract])))) **#3** ((((((((((((((((((((((((((((((((animal experimentation[MeSH Terms]) OR (models, animal[MeSH Terms])) OR (animals[MeSH Terms])) OR (animal population groups[MeSH Terms])) OR (animals, laboratory[MeSH Terms])) OR (animal*[Title/Abstract])) OR (rat[Title/Abstract])) OR (rats[Title/Abstract])) OR (mice[Title/Abstract])) OR (mouse[Title/Abstract])) OR (murine[Title/Abstract])) OR (rodent*[Title/Abstract])) OR (pig[Title/Abstract])) OR (pigs[Title/Abstract])) OR (rabbit*[Title/Abstract])) OR (dog[Title/Abstract])) OR (dogs[Title/Abstract])) OR (canine[Title/Abstract])) OR (goat*[Title/Abstract])) OR (monkey*[Title/Abstract])) OR (tibia*[Title/Abstract])) OR (radius[Title/Abstract])) OR (subcutaneous*[Title/Abstract])) OR	**#1** (TITLE-ABS KEY ("Titanium") OR TITLE-ABS-KEY ("Titania")) AND ((TITLE-ABS-KEY ("Coated materials, biocompatible") OR TITLE-ABS-KEY (coat*) OR TITLE-ABS-KEY (film*) OR TITLE-ABS-KEY (deposit*) OR TITLE-ABS-KEY ("surface treatment") OR TITLE-ABS-KEY ("surface treatments") OR TITLE-ABS-KEY ("surface treated") OR TITLE-ABS-KEY ("surfaces treated") OR TITLE-ABS-KEY ("treated surface") OR TITLE-ABS-KEY ("treated surfaces")) **#2** (TITLE-ABS KEY (antibiotic*) OR TITLE-ABS-KEY ("Amoxicillin") OR TITLE-ABS-KEY ("Penicillin") OR TITLE-ABS-KEY ("Azithromycin") OR TITLE-ABS-KEY ("Clarithromycin") OR TITLE-ABS-KEY (Anthracycline*) OR TITLE-ABS-KEY (Gentamicin*) OR TITLE-ABS-KEY ("Neomycin") OR TITLE-ABS-KEY ("Streptomycin") OR TITLE-ABS-KEY ("Streptozocin") OR TITLE-ABS-KEY ("Tobramycin") OR TITLE-ABS-KEY ("Vancomycin") OR TITLE-ABS-KEY ("Ciprofloxacin") OR TITLE-ABS-KEY ("Enrofloxacin") OR TITLE-ABS-KEY ("Clindamycin") OR TITLE-ABS-KEY ("Metronidazole") OR TITLE-ABS-KEY ("Doxycycline") OR TITLE-ABS-KEY ("Minocycline") OR TITLE-ABS-KEY ("Tetracycline"))) **#3** (TITLE-ABS-KEY ("animal experimentation") OR TITLE-ABS-KEY ("models, animal") OR TITLE-ABS-KEY ("animals") OR TITLE-ABS-KEY ("animal population groups") OR TITLE-ABS-KEY ("animals, laboratory") OR TITLE-ABS-KEY (animal*) OR TITLE-ABS-KEY ("rat") OR TITLE-ABS-KEY ("rats") OR TITLE-ABS-KEY ("mice") OR TITLE-ABS-KEY ("mouse") OR TITLE-ABS-KEY ("murine") OR TITLE-ABS-KEY (rodent*) OR TITLE-ABS-KEY ("pig") OR TITLE-ABS-KEY ("pigs") OR TITLE-ABS-	**#1** Topic: TS=("Coated materials, biocompatible" OR coat* OR film* OR deposit* OR surface* treat* OR treat* surface*) AND TS=(Antibiotic* OR "Amoxicillin" OR "Penicillin" OR "Azithromycin" OR "Clarithromycin" OR Anthracycline* OR Gentamicin* OR "Neomycin" OR "Streptomycin" OR "Streptozocin" OR "Tobramycin" OR "Vancomycin" OR "Ciprofloxacin" OR "Enrofloxacin" OR "Clindamycin" OR "Metronidazole" OR "Doxycycline" OR "Minocycline" OR "Tetracycline") **#2** Topic: TS=("animal experimentation" OR "models, animal" OR "animals" OR "animal population groups" OR "animals, laboratory" OR animal* OR "rat" OR "rats" OR "mice" OR "mouse" OR "murine" OR rodent* OR pig* OR rabbit* OR dog* OR "canine" OR goat* OR monkey* OR tibia* OR "radius" OR subcutaneous* OR calvaria* OR "calvarium" OR "femur" OR "jaw" OR mandible* OR palat* OR fibula* OR zygoma* OR "in vivo" OR "in situ" OR "clinical" OR "randomized" OR "nonrandomized" OR "non-randomized" OR "trial" OR intervention stud* OR "follow up" OR follow-up* OR patient* OR "human" OR volunteer* OR "quasi-experimental") **Topic: TS=(Titanium OR Titania) AND #1 AND #2**	**#1** MeSH descriptor: [Titanium] explode all trees **#2**(titanium):ti,ab,kw OR (titania):ti,ab,kw **#3 #1 OR #2** **#4** MeSH descriptor: [Coated materials, biocompatible] explode all trees 658 **#5** (coat*):ti,ab,kw OR (film):ti,ab,kw (deposit*):ti,ab,kw OR (surface* treat*):ti,ab,kw (treat* surface*):ti,ab,kw **#6 #4 OR #5** **#7** (antibiotic*):ti,ab,kw OR (amoxicillin):ti,ab,kw (Penicillin):ti,ab,kw OR (Azithromycin):ti,ab,kw (Clarithromycin):ti,ab,kw OR (Anthracycline*):ti,ab,kw (Gentamicin*):ti,ab,kw OR (Neomycin):ti,ab,kw (Streptomycin):ti,ab,kw OR (Streptozocin):ti,ab,kw (Tobramycin):ti,ab,kw OR (Vancomycin):ti,ab,kw (Ciprofloxacin):ti,ab,kw OR (Enrofloxacin):ti,ab,kw (Clindamycin):ti,ab,kw OR (Metronidazole):ti,ab,kw (Doxycycline):ti,ab,kw OR (Minocycline):ti,ab,kw (Tetracycline):ti,ab,kw **#8 #6 AND #7** **#9** MeSH descriptor: [Animal Experimentation] explode all trees **#10** MeSH descriptor: [Models, Animal] explode all trees **#11** MeSH descriptor: [Animal Population Groups] explode all trees	**#1** ('titanium'/exp/mj OR titanium:ti,ab,kw OR titania:ti,ab,kw) **#2** ('biocompatible coated material'/exp/mj OR coat*:ti,ab,kw OR film*:ti,ab,kw OR deposit*:ti,ab,kw OR 'surface* treat*':ti,ab,kw OR 'treat* surface*':ti,ab,kw) AND ('antibiotic agent'/exp/mj OR antibiotic:ti,ab,kw OR amoxicillin:ti,ab,kw OR penicillin:ti,ab,kw OR azithromycin:ti,ab,kw OR clarithromycin:ti,ab,kw OR anthracycline*:ti,ab,kw OR gentamicin*:ti,ab,kw OR neomycin:ti,ab,kw OR streptomycin:ti,ab,kw OR streptozocin:ti,ab,kw OR tobramycin:ti,ab,kw OR vancomycin:ti,ab,kw OR ciprofloxacin:ti,ab,kw OR enrofloxacin:ti,ab,kw OR clindamycin:ti,ab,kw OR metronidazole:ti,ab,kw OR doxycycline:ti,ab,kw OR minocycline:ti,ab,kw OR tetracycline:ti,ab,kw) **#3** ('animal experiment'/exp/mj OR 'animal model'/exp/mj OR 'animal'/exp/mj OR 'experimental animal'/exp/mj OR animal*:ti,ab,kw OR rat:ti,ab,kw OR rats:ti,ab,kw OR mice:ti,ab,kw OR mouse:ti,ab,kw OR murine:ti,ab,kw OR rodent*:ti,ab,kw OR pig:ti,ab,kw OR pigs:ti,ab,kw OR rabbit*:ti,ab,kw OR dog:ti,ab,kw OR dogs:ti,ab,kw OR canine:ti,ab,kw OR goat*:ti,ab,kw OR monkey*:ti,ab,kw OR tibia*:ti,ab,kw OR radius:ti,ab,kw OR subcutaneous*:ti,ab,kw OR	**#1** (Titanium OR Titania) **#2** (Coated materials, biocompatible OR coat* OR film* OR deposit* OR surface* treat*) **#3** (Antibiotic* OR Amoxicillin OR Penicillin OR Azithromycin OR Clarithromycin OR Anthracycline* OR Gentamicin* OR Neomycin OR Streptomycin OR Streptozocin OR Tobramycin OR Vancomycin OR Ciprofloxacin OR Enrofloxacin OR Clindamycin OR Metronidazole OR Doxycycline OR Minocycline OR Tetracycline) **#4** (animal experimentation OR models, animal OR animals OR animal population groups OR animals, laboratory OR animal* OR rat OR rats OR mice OR mouse OR murine OR rodent* OR pig* OR rabbit* OR dog* OR canine OR goat* OR monkey* OR tibia* OR radius OR subcutaneous* OR calvaria* OR calvarium OR femur OR jaw OR mandible* OR palat* OR fibula* OR zygoma* OR in vivo OR in situ OR clinical OR randomized OR nonrandomized OR non-randomized OR trial OR intervention stud* OR follow up OR follow-up* OR patient* OR human OR volunteer* OR quasi-experimental) **#1 AND #2 AND #3 AND #4**

(calvaria*[Title/Abstract])) OR (calvarium[Title/Abstract])) OR (femur[Title/Abstract])) OR (jaw[Title/Abstract])) OR (mandible*[Title/Abstract])) OR (palat*[Title/Abstract])) OR (fibula*[Title/Abstract])) OR (zygoma*[Title/Abstract])) OR (in vivo[Title/Abstract])) OR ((((((((((in situ[Title/Abstract]) OR (clinical[Title/Abstract])) OR (randomized[Title/Abstract])) OR (nonrandomized[Title/Abstract])) OR (non-randomized[Title/Abstract])) OR (trial[Title/Abstract])) OR (intervention stud*[Title/Abstract])) OR (follow up[Title/Abstract])) OR (follow-up*[Title/Abstract])) OR (patient*[Title/Abstract])) OR (human[Title/Abstract])) OR (volunteer*[Title/Abstract])) OR (quasi-experimental[Title/Abstract]))) **#1 AND #2 AND #3**	KEY (rabbit*) OR TITLE-ABS-KEY ("dog") OR TITLE-ABS-KEY ("dogs") OR TITLE-ABS-KEY ("canine") OR TITLE-ABS-KEY (goat*) OR TITLE-ABS-KEY (monkey*) OR TITLE-ABS-KEY (tibia*) OR TITLE-ABS-KEY ("radius") OR TITLE-ABS-KEY (subcutaneous*) OR TITLE-ABS-KEY (calvaria*) OR TITLE-ABS-KEY ("calvarium") OR TITLE-ABS-KEY ("femur") OR TITLE-ABS-KEY ("jaw") OR TITLE-ABS-KEY (mandible*) OR TITLE-ABS-KEY (palat*) OR TITLE-ABS-KEY (fibula*) OR TITLE-ABS-KEY (zygoma*) OR TITLE-ABS-KEY ("in vivo") OR TITLE-ABS-KEY ("in situ") OR TITLE-ABS-KEY ("clinical") OR TITLE-ABS-KEY ("randomized") OR TITLE-ABS-KEY ("nonrandomized") OR TITLE-ABS-KEY ("non-randomized") OR TITLE-ABS-KEY ("trial") OR TITLE-ABS-KEY ("intervention study") OR TITLE-ABS-KEY ("intervention studies") OR TITLE-ABS-KEY ("follow up") OR TITLE-ABS-KEY (follow-up*) OR TITLE-ABS-KEY (patient*) OR TITLE-ABS-KEY ("human") OR TITLE-ABS-KEY (volunteer*) OR TITLE-ABS-KEY ("quasi-experimental")) **#1 AND #2 AND #3**		**#12** MeSH descriptor: [Animals, Laboratory] explode all trees **#13** MeSH descriptor: [Animals] explode all trees **#14** (animal*):ti,ab,kw OR (rat):ti,ab,kw (rats):ti,ab,kw OR (mice):ti,ab,kw OR (mouse):ti,ab,kw OR (murine):ti,ab,kw (rodent*):ti,ab,kw OR (pig):ti,ab,kw OR (pigs):ti,ab,kw OR (rabbit*):ti,ab,kw (dog):ti,ab,kw OR (dogs):ti,ab,kw OR (canine):ti,ab,kw OR (goat*):ti,ab,kw (monkey*):ti,ab,kw OR (tibia*):ti,ab,kw OR (radius):ti,ab,kw OR (subcutaneous*):ti,ab,kw (calvaria*):ti,ab,kw OR (calvarium):ti,ab,kw OR (femur):ti,ab,kw OR (jaw):ti,ab,kw (mandible*):ti,ab,kw OR (palat*):ti,ab,kw OR (fibula*):ti,ab,kw OR (zygoma*):ti,ab,kw (in vivo):ti,ab,kw OR (in situ):ti,ab,kw OR (clinical):ti,ab,kw OR (randomized):ti,ab,kw OR (nonrandomized):ti,ab,kw (non-randomized):ti,ab,kw OR (trial):ti,ab,kw OR (intervention stud*):ti,ab,kw OR (follow up):ti,ab,kw (follow-up*):ti,ab,kw OR (patient*):ti,ab,kw OR (human):ti,ab,kw OR (volunteer*):ti,ab,kw OR (quasi-experimental):ti,ab,kw **#15 #9 OR #10 OR #11 OR #12 OR #13 OR #14**	calvaria*:ti,ab,kw OR calvarium:ti,ab,kw OR femur:ti,ab,kw OR jaw:ti,ab,kw OR mandible*:ti,ab,kw OR palat*:ti,ab,kw OR fibula*:ti,ab,kw OR zygoma*:ti,ab,kw OR 'in vivo':ti,ab,kw OR 'in situ':ti,ab,kw OR clinical:ti,ab,kw OR randomized:ti,ab,kw OR nonrandomized:ti,ab,kw OR 'non randomized':ti,ab,kw OR trial:ti,ab,kw OR 'intervention stud*':ti,ab,kw OR 'follow up':ti,ab,kw OR 'follow up*':ti,ab,kw OR patient*:ti,ab,kw OR human:ti,ab,kw OR volunteer*:ti,ab,kw OR 'quasi experimental':ti,ab,kw) **#1 AND #2 AND #3**	

TABLE S2 - Summary of excluded studies, related to the main text and Figure 6.

Reason for exclusion	Number	Studies
Does not used titanium-based implants	2	Bernthal et al. (2010); Jennings et al. (2015)
Does not evaluate microbial colonization quantitatively on implant surface	18	Vester et al. (2010); Norowski et al. (2011); Stewart et al. (2012); Qu et al. (2014); Walter et al. (2014); Zhang et al. (2014); Nast et al. (2016); Li et al. (2017, 2018, 2020); Schmidmaie et al. (2017); Wan et al. (2017); Sutrisno et al. (2018); Li et al. (2019); Qian et al. (2019); Williams et al. (2019); Sumathra et al. (2020); Yavari et al. (2020).
Microbiological evaluation in bone tissue only	4	Moojen et al. (2009); Yang et al. (2013); Ma et al. (2017); Boot et al. (2020).
Human study without control group	1	Fuchs et al. (2011)
Unavailable full text	2	Liu et al. (2016); Wang et al. (2017)
Other reasons	6	Ren et al. (2014); Liu et al. (2016); Nast et al. (2016a); Nast et al. (2016b); Qu et al. (2016); Zhang et al. (2018).

REFERENCES

Bernthal, N.M., Stavrakis, A.I., Billi, F., et al. (2010). A mouse model of post-arthroplasty Staphylococcus aureus joint infection to evaluate in vivo the efficacy of antimicrobial implant coatings. PLoS One. 5, e12580.

Burda, B.U., O'Connor, E.A., Webber, et al. (2017). Estimating data from figures with a web-based program: considerations for a systematic review. Res. Synth. Methods 8, 258–262.

Boot, W., Vogely, H.C., Jiao, C., et al. (2020). Prophylaxis of implant-related infections by local release of vancomycin from a hydrogel in rabbits. Eur Cell Mater. 39, 108-120.

Fuchs, T., Stange, R., Schmidmaier, G., Raschke, M.J. (2011). The use of gentamicin-coated nails in the tibia: preliminary results of a prospective study. Arch Orthop Trauma Surg. 131,1419-1425.

Jennings, J.A., Carpenter, D.P., Troxel, K.S., et al. (2015). Novel Antibiotic-loaded Point-of-care Implant Coating Inhibits Biofilm. Clin Orthop Relat Res. 473, 2270-2282.

Li, D., Lv, P., Fan, L., et al. (2017). The immobilization of antibiotic-loaded polymeric coatings on osteoarticular Ti implants for the prevention of bone infections. Biomater Sci. 5,2337-2346.

Li, H., Nie, B., Zhang, S., Long, T., Yue, B. (2019). Immobilization of type I collagen/hyaluronic acid multilayer coating on enoxacin loaded titania nanotubes for improved osteogenesis and osseointegration in ovariectomized rats. Colloids Surf B Biointerfaces. 175,409-420.

Li, Y., Li, L., Ma, Y., et al. (2020). 3D-Printed Titanium Cage with PVA-Vancomycin Coating Prevents Surgical Site Infections (SSIs). Macromol Biosci. 20, e1900394.

Ding, L., Zhang, P., Wang, X., et al. (2019) Effect of doxycycline-treated hydroxyapatite surface on bone apposition: A histomophometric study in murine maxillae. Dent Mater J. 37, 130-138.

Ma, K., Cai, X., Zhou, Y., Wang, Y., Jiang, T. (2017). In Vitro and In Vivo Evaluation of Tetracycline Loaded Chitosan-Gelatin Nanosphere Coatings for Titanium Surface Functionalization. Macromol Biosci. 17, 10.1002/mabi.201600130.

Moojen, D.J., Vogely, H.C., Fleer, A., et al. (2009). Prophylaxis of infection and effects on osseointegration using a tobramycin-periapatite coating on titanium implants--an experimental study in the rabbit. J Orthop Res. 27, 710-716.

Nast, S., Fassbender, M., Bormann, N., et al. (2016). In vivo quantification of gentamicin released from an implant coating. J Biomater Appl. 31, 45-54.

Nast, S., Fassbender, M., Bormann, N., et al. (2016). Quantification and analysis of local gentamicin release in vitro and in an animal model. J Orthop Res. 34, 157.
Norowski, P.A., Courtney, H.S., Babu, J., Haggard, W.O., Bumgardner, J.D. (2011). Chitosan coatings deliver antimicrobials from titanium implants: a preliminary study. Implant Dent. 20, 56-67.

Qiu, J., Qian, W., Zhang, J., Chen, D. et al. (2019). Minocycline hydrochloride loaded graphene oxide enables enhanced osteogenic activity in the presence of Gram-positive bacteria, Staphylococcus aureus. J. Mater. Chem. B. 7, 3590-3598.

Qu, H., Knabe, C., Burke, M., et al. (2014). Bactericidal micron-thin sol-gel films prevent pin tract and periprosthetic infection. Mil Med. 179(8 Suppl), 29-33.

Qu, H. (2016). Micron-Thin Bactericidal sol-gel films for the treatment of periprosthetic infection–a 3-month ovine study. J Orthop Res. 34, 112.

Ren, W., Song, W., Markel D. (2014). Implant Infection Was Controlled by Sustained Release
of Doxycyclin From a Nanofiber Coating. Tissue Eng Part A 20, S-4.

Qian, W., Qiu, J., Liu, X. (2020). Minocycline hydrochloride-loaded graphene oxide films on implant abutments for peri-implantitis treatment in beagle dogs. J Periodontol. 2020;91(6):792-799.

Stewart, S., Barr, S., Engiles, J., et al. (2012). Vancomycin-modified implant surface inhibits biofilm formation and supports bone-healing in an infected osteotomy model in sheep: a proof-of-concept study. J Bone Joint Surg Am. 94,1406-1415.

Sutrisno, L., Wang, S., Li, M., et al. (2018). Construction of three-dimensional net-like polyelectrolyte multilayered nanostructures onto titanium substrates for combined antibacterial and antioxidant applications. J. Mater. Chem. B**.** 6**,** 5290-5302.

Sumathra, M., Rajan, M., Praphakar, R.A., Marraiki, N., Elgorban, M. A. (2020). In Vivo Assessment of a Hydroxyapatite/κ-Carrageenan–Maleic Anhydride–Casein/Doxorubicin Composite-Coated Titanium Bone Implant. ACS Biomater. Sci. Eng. 6, 1650–1662.

Schmidmaier, G., Kerstan, M., Schwabe, P., Südkamp, N., Raschke, M. (2017). Clinical experiences in the use of a gentamicin-coated titanium nail in tibia fractures. Injury. 48, 2235-2241.

Vester, H., Wildemann, B., Schmidmaier, G., Stöckle, U., Lucke, M. (2010). Gentamycin delivered from a PDLLA coating of metallic implants: In vivo and in vitro characterisation for local prophylaxis of implant-related osteomyelitis. Injury. 41, 1053-1059.

Walter, M.S., Frank, M.J., Satué, M., et al. (2014). Bioactive implant surface with electrochemically bound doxycycline promotes bone formation markers in vitro and in vivo. Dent Mater. 30, 200-214.

Wan, M., Zhang, J., Wang, Q., et al. (2017). In Situ Growth of Mesoporous Silica with Drugs on Titanium Surface and Its Biomedical Applications. ACS Appl Mater Interfaces. 9, 18609-18618.

Wang, Y., Wan, Y., Zhang X., Ye, J., Zhuo, N. (2017). Titanium intramedullary nail coated with vancomycin-hydroxyapatite in a model of open long bone fracture with wound infection. Chinese J Tissue Eng Res. 21, 2163-2169.

Williams, D.L., Epperson, R.T., Ashton, N.N., et al. (2019). In vivo analysis of a first-in-class tri-alkyl norspermidine-biaryl antibiotic in an active release coating to reduce the risk of implant-related infection. Acta Biomater. 93, 36-49.

Yang, C.C., Lin, C.C., Liao, J.W., Yen, S.K. (2013). Vancomycin-chitosan composite deposited on post porous hydroxyapatite coated Ti6Al4V implant for drug controlled release. Mater Sci Eng C Mater Biol Appl. 33, 2203-2212.

Yavari, S.A., Croes M., Akhavan, B. et al. (2020). Layer by layer coating for bio-functionalization of additively manufactured meta-biomaterials. Additive Manufacturing. 32, 100991.

Zhang, L., Yan, J., Yin, Z., et al. (2014). Electrospun vancomycin-loaded coating on titanium implants for the prevention of implant-associated infections. Int J Nanomedicine. 9,3027-3036.

Zhang, S., Cheng, X., Shi, J., et al. (2018b). Electrochemical Deposition of CalciumPhosphate/Chitosan/Gentamicin on a Titanium Alloy for Bone Tissue Healing. Int J Electrochem Sci. 13, 4046 – 4054.